

# A new Early Paleogene fossil mammal locality in the central-eastern Nemegt Basin, Gobi Desert, Mongolia, and notes on mammalian biostratigraphy

Khand Yo,<sup>1</sup> Eva A. Hoffman,<sup>2,3</sup> Maureen A. O’Leary,<sup>3,4\*</sup>  and Michael J. Novacek<sup>3</sup>

<sup>1</sup>Institute of Paleontology, Mongolian Academy of Sciences (MAS), Chingeltei district-4, S. Danzan Street 3/1, Ulaanbaatar-15160, Mongolia <[khandpaleo@gmail.com](mailto:khandpaleo@gmail.com)>

<sup>2</sup>Richard Gilder Graduate School, American Museum of Natural History, New York, New York, 10024, USA <[ehoffman@amnh.org](mailto:ehoffman@amnh.org)>

<sup>3</sup>Division of Paleontology, American Museum of Natural History, New York, New York, 10024, USA <[novacek@amnh.org](mailto:novacek@amnh.org)>

<sup>4</sup>Department of Anatomical Sciences, Renaissance School of Medicine, Stony Brook University, Stony Brook, New York, 11794-8081, USA <[maureen.oleary@stonybrook.edu](mailto:maureen.oleary@stonybrook.edu)>

---

**Abstract.**—We report new, fossiliferous Paleogene Naran Bulak Formation localities from the central-eastern part of the Nemegt Basin of the Gobi Desert, Mongolia. Early Paleogene localities have been identified previously only in the western half of the Nemegt Basin. The new localities, near the town of Daus, are also noteworthy for their geographical proximity to Ukhaa Tolgod, a Late Cretaceous Djadokhta Formation locality known for its numerous dinosaur, mammal, and lizard fossils. The Daus section consists of the Zhigden, Naran, and Bumban members of the Naran Bulak Formation at three localities, and mammal and ostracode fossils were discovered in the Naran Member. Noteworthy discoveries are a dentary of the pantodont *Archaeolambda* cf. *A. planicanina*, postcrania of *Pantolambdodon*, a skull of the gliroid *Gomphos*, and a partial skull with a worn and damaged dentition provisionally identified as an arctostylopid. Biostratigraphy has been the primary means of dating Paleogene Asian faunas, however, the local fauna from the new localities does not fit easily with established patterns. The Naran Member and *Archaeolambda planicanina* and the arctostylopid *Palaeostylops* typically have been allied with the Gashatan Asian Land Mammal Age (ALMA) and attributed to the latest Paleocene. By contrast, *Gomphos* repeatedly has been found in the Bumban Member and assigned a Bumbanian ALMA, which has been considered as the earliest Eocene. *Pantolambdodon* has been reported from middle Eocene Arshatan and Irдинmanhan ALMA beds. The co-occurrence of these taxa in Naran Member beds complicates the temporal interpretation of the new localities and the reliability of broader biostratigraphic patterns.

---

## Introduction

Since the late 1960s, joint Mongolian-Russian and Mongolian-Polish paleontological expeditions have contributed greatly to the characterization of Cenozoic stratigraphy and paleontology in Mongolia (see review in Lopatin, 2020). Detailed descriptions of stratigraphic and paleontological evidence from localities in the region of the Nemegt Basin, known as Naran Bulak (Fig. 1), and exposures farther west at Tsagan Khushu have led to the characterization of the Naran Bulak Formation in the region directly south of the Altan Mountains (Altan Uul). This formation is a terrestrial series of sandstones, clays, and carbonates that has been interpreted as having lacustrine and fluvial sediments (Dashzeveg, 1988; Meng et al., 1998).

Until now, the Naran Bulak Formation has been identified only in the western part of the Nemegt Basin (Dashzeveg, 1988, fig. 1), however, we show that the central-eastern region of the Nemegt Basin also contains Naran Bulak Formation exposures.

Our discovery occurred during extensive paleontological expeditionary work conducted at the highly fossiliferous locality Ukhaa Tolgod. Discovered in 1993 by a Mongolian Academy-American Museum Paleontological Expedition (MAE), this Upper Cretaceous Djadokhta Formation locality is noteworthy for its numerous, well-preserved dinosaur skeletons, embryos, and eggs, as well as fossil mammals, lizards, and other vertebrates (Norell et al., 1994; Dashzeveg et al., 1995; Novacek et al., 1997; Clark et al., 1999). Beginning in 1993, outcrops of stratigraphically higher rocks located 12 km to the southwest of the main section at Ukhaa Tolgod were first prospected (Fig. 1).

This more southerly unit initially appeared to be unfossiliferous until the 2014–2015 Mongolian Academy-American Museum of Natural History field seasons when the team discovered ostracodes and fragmentary teeth and bones of mammals. Subsequently, in 2017 and 2019, a concentration of mammalian fossils, including identifiable jaws and dentitions, were found in white beds at three localities, Daus-1, Daus-2a, and Daus-2b, located near the town of Daus in the Omnigov Imac province (Figs. 1–3). The sedimentary features, color, and stratification

---

\*Corresponding author.

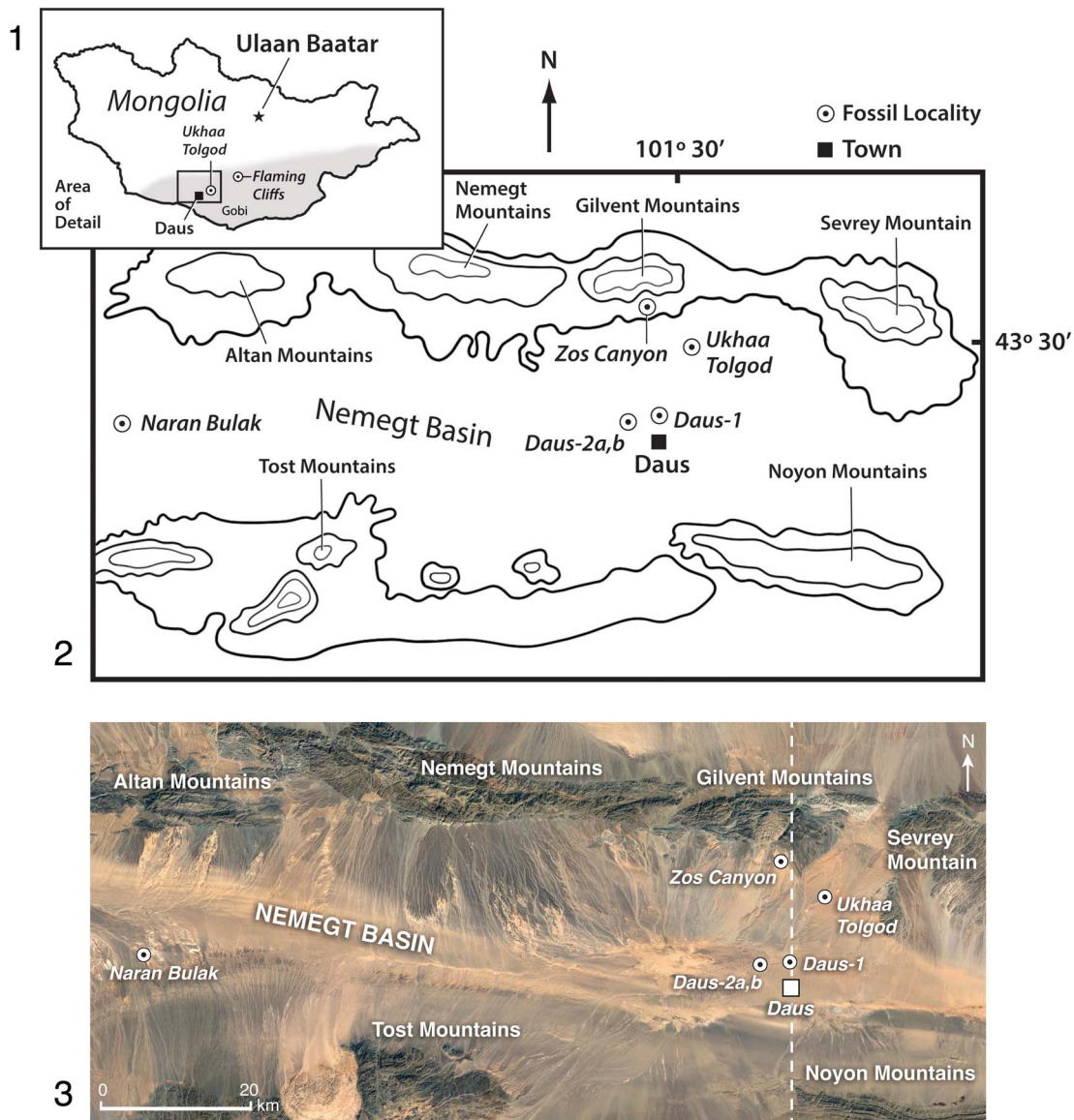


**Figure 1.** (1) Map of Mongolia and the Gobi Desert (gray shading) where the new fossils were found; boxed area is expanded in (2, 3). (2) Map of Nemegt Basin and adjacent mountains showing fossil localities (italicized text) relative to nearby towns; and (3) the same region shown as a Google Earth satellite image that reveals the relief of the localities and their south-trending exposure; dotted line is the transect shown in Figure 3. New Paleogene localities are Daus-1, Daus-2a, and Daus-2b, which are near the highly productive Late Cretaceous locality Ukhaa Tolgod. The locality Zos Canyon extends east from where it is marked in (2) and the locality Ukhaa Tolgod extends southwest. The type locality of the Paleogene Naran Bulak Formation is separated from the Daus localities by ~90 km. The Late Cretaceous locality Ukhaa Tolgod indicated is described elsewhere (Pol and Norell, 2004; Dingus et al., 2008).

of the section at these new localities resemble those of the type section of the Naran Bulak Formation, and the specific fossil-yielding white beds we found correspond to the Naran Member of the Naran Bulak (Fig. 2; Dashzeveg, 1988). Lopatin (2020) summarized the vertebrate fossils that have been recovered from the western exposures of the Naran Member (“White Beds”), including amiid fishes, crocodyliforms, aves, and mammals such as archaeolambdids, arctostyloids, multituberculates, mesonychia, coryphodontids, and the rodent *Tribosphenomys*, among other taxa.

Due to a lack of marine and volcanic deposits in Central Asian regions, including the Nemegt Basin of the Gobi Desert, Mongolia (Dashzeveg, 1988; Meng et al., 1998; Ting, 1998; Dingus et al., 2008), the age estimate of the Naran Bulak

Formation has been limited to biostratigraphy (Gradziński, 1969; Szczechura, 1971; Dashzeveg and McKenna, 1977; Dashzeveg, 1982, 1988; Khand, 1987; Beard, 1998; Lucas, 1998; Wang et al., 2010). The Naran Bulak Formation is thought to represent two key Asian Land Mammal Ages (ALMAs): the Gashatan and the Bumbanian, with the former historically considered to be of latest Paleocene age and the latter generally considered the earliest Eocene (Dashzeveg, 1982, 1988; Russell and Zhai, 1987; Ting, 1998). More recent assessments, including those that tied biostratigraphy to magnetostratigraphy and chemostratigraphy, showed that while the Gashatan ALMA was entirely Paleocene, the Bumbanian ALMA may contain the Paleocene-Eocene boundary (Meng et al., 1998; Bowen et al., 2002; Ting et al., 2003, fig. 4). However, Bowen et al. (2005)

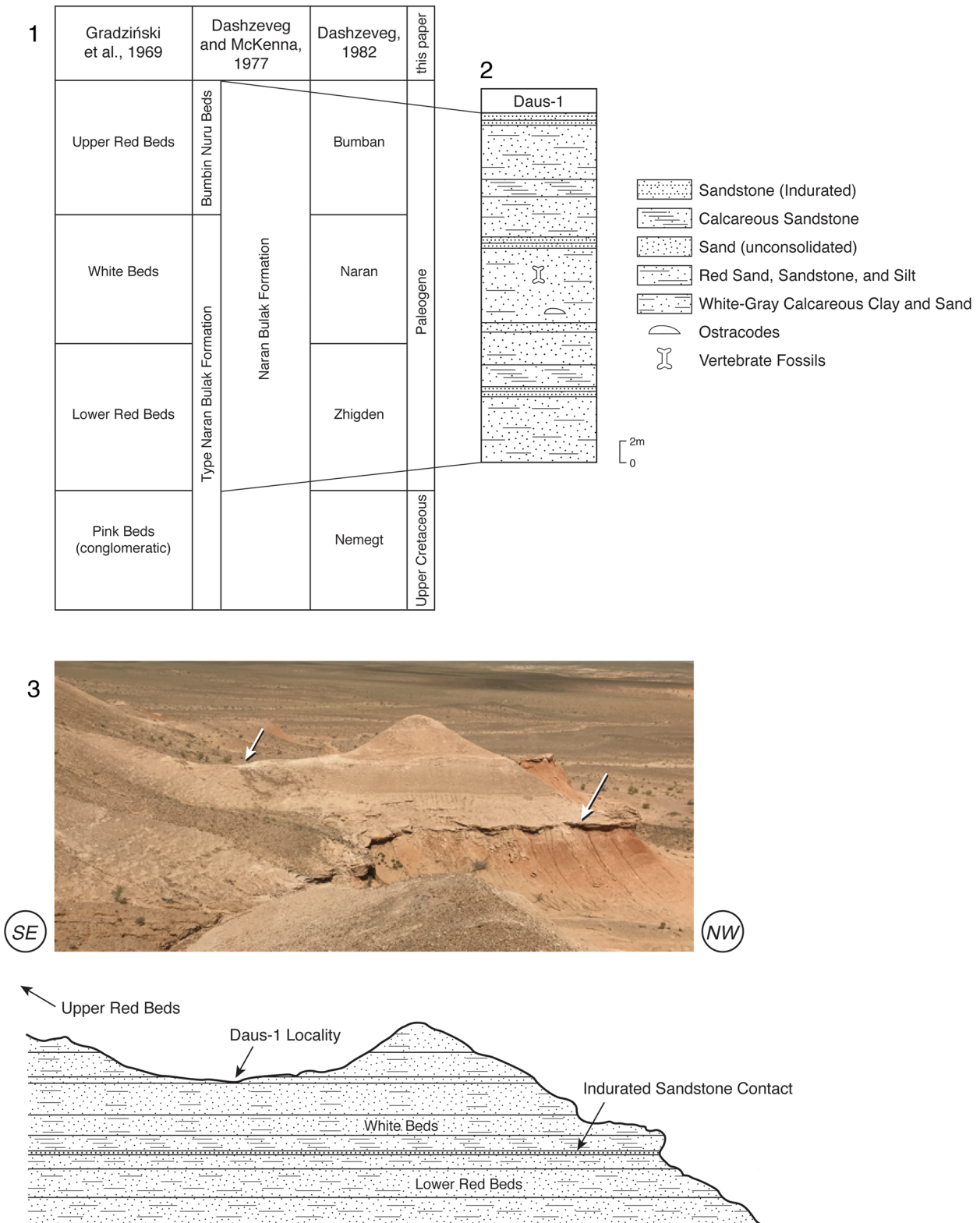


**Figure 2.** (1) Naran Bulak Formation stratigraphy. Fossils described here come from the Naran Member (“White Beds”) of this formation. Three sections are summarized. The section described by Gradziński (1969) was later designated the type section by Dashzeveg and McKenna (1977), who specified that although the Upper Red Beds are not found in the Gradziński (1969) section, they are to be included in the type Naran Bulak Formation. Dashzeveg (1982) provided names for the Naran Bulak Formation members. Discussions in these papers reveal disagreement over whether the upper part of the Naran Bulak Formation is Paleocene or Eocene. We treat the Zhigden, Naran, and Bumban beds as Paleogene for lack of additional temporal control. (2) Our ~30 m section at the Daus-1 locality representing all of the same Naran Bulak beds as the type section, except the lowest, conglomeratic “Pink Beds.” (3) Photograph of the Daus-1 locality with an explanatory schematic below indicating the Daus-1 locality within the Naran Member (“White Beds”) above an indurated sandstone that we interpret as a channel deposit. The part of section visible in the photograph is ~19 m high.



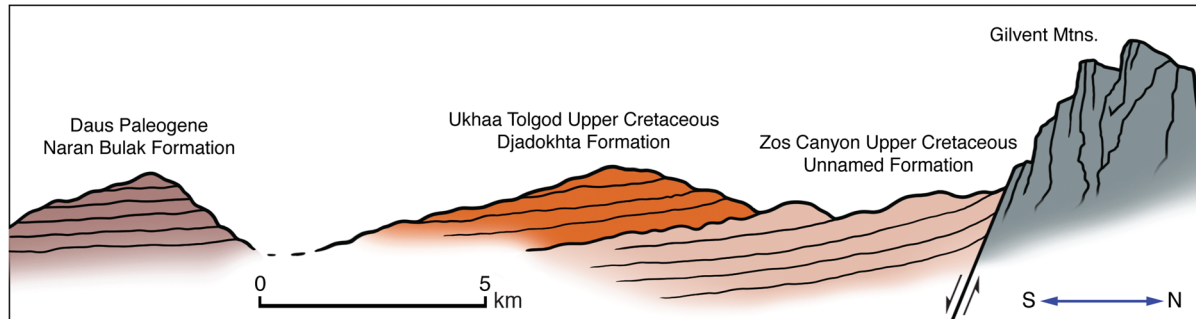


**Figure 3.** Schematic showing cross-section of the Naran Bulak Formation lying unconformably on the Upper Cretaceous Djadokhta Formation, which in turn overlies an older, unnamed Upper Cretaceous formation exposed in Zos Canyon (Pol and Norell, 2004).

refined this hypothesis with new data indicating that the Gashatan ALMA persisted close to the Paleocene-Eocene boundary.

Below we describe for the first time the general lithology and paleontology of three Naran Bulak Formation localities found >90 km east of the Naran Bulak Formation type section (Gradziński et al., 1969; Dashzeveg and McKenna, 1977; Dashzeveg, 1988). The fossil occurrences at this site and the extensive lateral exposure of this unit indicate that there is a much more widespread distribution of Paleogene rocks in the Nemegt Basin south of the Altan, Nemegt, and Gilvent mountains than previously known (Figs. 1, 2).

## Geological setting

*Geological time unit.*—Early Paleogene (Fig. 2).

*Stratigraphic information.*—The lithology of the three new localities (Daus-1, Daus-2a, Daus-2b) is geologically consistent with published accounts of the Naran Bulak Formation that crop out in the western Gobi Desert (Dashzeveg, 1968; Gradziński et al., 1969; Shuvalov et al., 1974; Shishkin, 1975; Badamgarav and Reshetov, 1985; Bekhbat et al., 1999). Gradziński (1969) described the western Nemegt Basin Paleogene rocks at Naran Bulak, but did not explicitly name a type section. Subsequently, Dashzeveg and McKenna (1977) recognized the section described by Gradziński (1969, fig. 12) as the Naran Bulak Formation type section, comprising, from lowest to highest, the conglomeratic “Pink Beds,” the “Lower Red Beds,” and the “White Beds.” Dashzeveg and McKenna (1977) additionally recognized an upper unit, the “Upper Red Beds” of Gradziński et al. (1969), as the Bumbin-Nuru beds, which are referable to the type section of the Naran Bulak Formation even though such beds are not in the region of the type section (Dashzeveg and McKenna, 1977, fig. 2). Dashzeveg (1988) later recognized the “Lower Red Beds” as the Zhigden Member, the “White Beds” as the Naran Member, and the “Upper Red Beds” as the Bumban Member, all of the Naran Bulak Formation. The unit below the Zhigden Member, the conglomeratic “Pink Beds” included in the Naran Bulak Formation by Dashzeveg and McKenna (1977), was later recognized by Dashzeveg (1988, fig. 2) as a unit within the Cretaceous Nemegt Formation, a designation we follow here (Fig. 2). Dashzeveg (1982) also added, with reservation, an additional youngest

member to the Naran Bulak Formation, the Aguyt, which has a poorly characterized fauna, and we do not discuss it further here.

According to Dashzeveg (1988, p. 473), the beds in the Naran Bulak area, where the type section is located, have 80 m of “alternating sandstones and clays, with intercalations of light grey carbonates; light grey and red colors predominate. The strata are horizontal and cross-bedding occurs” (see also Dashzeveg, 1982). These Naran Bulak area rocks lie unconformably over the Cretaceous “Upper Nemegt Beds,” whose lithology was described extensively by Gradziński (1969). The lithological characterization of the type section of the Naran Bulak Formation is consistent with the stratigraphy at Daus-1, Daus-2a, and Daus-2b, although at Daus-1 the exposure is ~30 m (at Daus-2a and Daus-2b, the total section height has not yet been measured). At the Daus-1 locality there are lower red, middle white, and upper red beds, as have been described for the Naran Bulak Formation type section (Fig. 2; Gradziński et al., 1969; Dashzeveg and McKenna, 1977), that extend laterally for ~2 km. The lower red beds at Daus-1 consist primarily of coarse-grained sandstones and aleurite. The middle white beds consist of white to gray calcareous clay and equigranular sands. The upper red strata contain aleurite and inequigranular sands and sandstone. The Naran Member (“White Beds”), which yielded the new fossils, historically has been a very fossiliferous part of the section in the type region of Naran Bulak (Dashzeveg and McKenna, 1977; Dashzeveg, 1988; Lopatin, 2020).

At the Daus localities, there is no evidence of exposures comparable to the Cretaceous Upper Nemegt Beds of Gradziński (1969) that unconformably underlie the type section of the Naran Bulak Formation. The nearest Cretaceous exposures lie ~1 km to north at Ukhaa Tolgod, a section described as the Upper Cretaceous Djadokhta Formation (Dingus et al., 2008). The angle and direction of dip of the Ukhaa Tolgod section suggest that the Naran Bulak Formation at Daus rests unconformably on it (Fig. 3). The relationship of the Ukhaa Tolgod section to the younger Naran Bulak section at Daus, however, is not yet clear because the units are separated by a broad wash covered by surface pediment and vegetation.

*Locality information.*—We present data on three new localities. The coordinates for locality Daus-1 are 43°27′20″N, 101°28′56″E in the central part of the greater Nemegt Basin,

~14.5 km south of the Gilvent Mountains of the Gurvan Tesoum (a small administrative unit under the Omnogov imac or “province”), Mongolia. Daus-1 is 10 km northwest of a salt factory at the town of Daus and 90 km east of the type Naran-Bulak section. The localities Daus-2a and Daus-2b, are located at 43°26′14″N, 101°26′17″E and 43°26′53″N; 101°26′41″E, respectively. Daus-2a and Daus-2b lie ~3 km and ~4 km, respectively, to west-southwest of Daus-1. The section at these localities is essentially the same as that described above for Daus-1, although the lower red beds assigned to the Zhigden Member at Daus-2a and Daus-2b are more poorly exposed, being confined to low hills and gullies at the base of the cliffs.

**Biostratigraphy.**—As noted above, biostratigraphy based on fossil mammals has been the primary means of dating the Naran Bulak Formation. Fossil mammals also have been the foundation of more comprehensive efforts to establish Asian Land Mammal Ages (ALMAs; the origins of these terms are reviewed in Lucas, 1998) to correlate terrestrial sediments within Asia and more broadly among Asian localities and those in Europe and North America. The two ALMAs most directly relevant to the new Daus localities are the Gashatan ALMA, in which the Zhigden and Naran members occur, and the Bumbanian ALMA, in which the Bumban Member occurs (Ting, 1998).

A few key points from prior literature are most relevant to our work. The Zhigden and Naran members have been assigned to the Gashatan ALMA because they contain such taxa such *Tribosphenomys*, *Arctostylops*, *Prodinoceras*, and *Archaeolambda planicanina* Flerov, 1952. Of these taxa, only *Arctostylops* is found outside of Asia and, although the genus once served as an index taxon supporting the direct assignment of these beds to the Paleocene (Dashzeveg, 1982, fig. 2, p. 278; Lucas, 1998, fig. 21.22, p. 479), this role for the taxon has not withstood taxonomic reassessment. The Asian *Arctostylops* species, *A. iturus* Dashzeveg and Russell, 1988, has been re-assigned to *Palaeostylops iturus* Matthew and Granger, 1925 (Cifelli et al., 1989; Kondrashov and Lucas, 2004), a species originally described by Matthew and Granger (1925) from the Gashatan beds near Bayn Dzak (“the Flaming Cliffs,” see Fig. 1) and not known outside Asia. *Archaeolambda planicanina* Flerov, 1952, also may be found consistently in, and be a signature for, the Gashatan beds (Lopatin, 2020), but it can only provide age data by proxy because it is not known from radiometrically dated rocks outside of Asia (note also that Dashzeveg [1988, fig. 4] reported its rare occurrence in Bumbanian beds, complicating matters further). The signature Gashatan taxon, *Tribosphenomys*, the first Asian appearance of the mammalian order Rodentia (Ting, 1998, p. 131), is similarly constrained. Based on a combination of magnetostratigraphy, chronostratigraphy, and biostratigraphy, the Gashatan ALMA is currently considered Paleocene (Meng et al., 1998; Bowen et al., 2002, 2005).

The Bumban Member has been assigned to the Bumbanian ALMA because it contains the taxa *Orientolophus*, *Prodinoceras*, *Gomphos*, *Homogalax*, and *Hyopsodus*, the latter two being truly Holarctic genera that appeared in the Eocene and are known from radiometrically dated sediments in North America (Woodburne and Swisher III, 1995, fig. 1). Dashzeveg

(1982, p. 277) mentioned the occurrence of *Arctostylops* in the Bumban Member of the Naran Bulak Formation of Mongolia, but this record has never been confirmed (Wang et al., 2008). *Arctostylops* has not been reported in either the Gashatan or Bumbanian deposits in recent taxonomic compilations (Lopatin, 2020). Ting (1998) argued that the appearance of the ceratomorph *Orientolophus* in the Bumbanian marked the first Asian appearance of the mammalian order Perissodactyla and was a useful biostratigraphic indicator. Bai et al. (2018) more recently showed that as many as four distinct perissodactyl clades (equids, ceratomorphs, ancylopods, and brontotheres) appear to have been present in the early Eocene of Asia, but this discovery has yet to be used broadly for biostratigraphy. *Gomphos*, which is endemic to Asian rocks, also has been recognized as a signature for the Bumbanian ALMA. Knowledge of the actual age of *Gomphos*, however, currently derives from its association with *Hyopsodus* and *Homogalax*, a point noted by Dashzeveg (1988, p. 474, 477). The Bumbanian ALMA is considered primarily Eocene, but also may contain the Paleocene-Eocene boundary (Meng et al., 1998; Bowen et al., 2002, 2005).

Finally, although microfossils are known from the Naran Bulak Formation, Dashzeveg and McKenna (1977, p. 125–126) emphasized that such fossils have not been particularly useful index taxa because they are either too geographically localized or they lacked well-understood and restricted stratigraphic ranges. It is noteworthy, however, that the ostracode *Limnocythere nemegtensis* Szczechura, 1971, which we report on here, recently has been recovered from Paleocene beds in China, strengthening its role as a signature taxon within Asia (Zhao, 1985; Wang et al., 2019). Later work showed that the ostracode fauna confirmed, to a certain extent, a late Paleocene age for the Zhigden and Naran members of the Naran-Bulak Formation and an early Eocene age for the the Bumban Member (Khand, 1987).

**Fossils discovered and depositional environment.**—Among the collected fossils are dentitions, skulls, and postcrania. Many of these elements are fragmentary and exhibit postmortem damage, thus we describe here those exhibiting diagnostic features. The gray-colored, sandy-clay composition of the Naran Bulak beds previously has been interpreted as lower alluvial and upper lacustrine horizons (Dashzeveg, 1988).

## Materials and methods

**Taphonomy and preparation.**—The vertebrate and ostracode specimens were surface-collected from the white-gray calcareous clay and sand as in situ fossils, not as float, from the Naran Member (“White Beds” described above). The specimens, for the most part, were not found in lenses, as has been reported for more westerly localities of the Naran Bulak Formation (Dashzeveg, 1988, fig. 2), although the fossils found at Daus-2b are possibly preserved in a thin, very restricted facies. Several fossil mammal specimens received manual preparation. The ostracode samples were immersed in water for 5–6 hours, then washed through sieves (500, 250, and 125µm). Ostracode specimens that were well preserved and particularly complete were selected for examination under

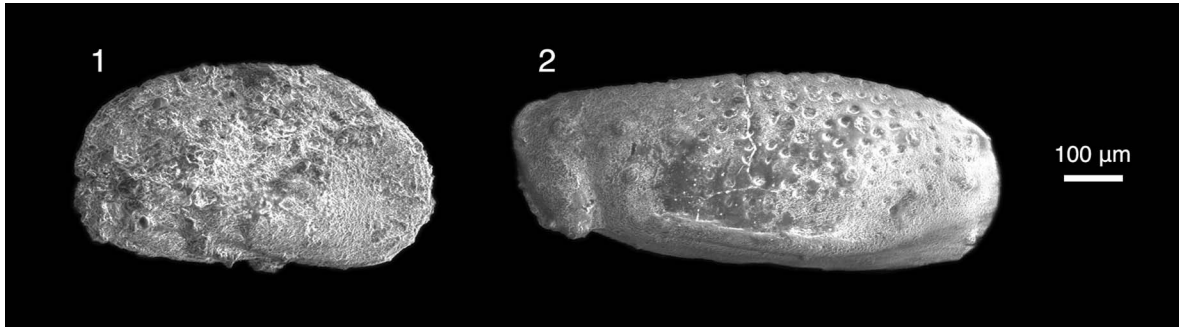


**Figure 4.** Freshwater Ostracoda from the locality Daus-1, collected in the Naran Member of the Naran Bulak Formation, western Gobi Desert, Mongolia. (1) *Limnocythere nemegtensis* Szczechura, 1971 (N 5/69a PIN MAS). (2) Cyprideidae genus and species indet., (N 5/69b PIN MAS), left valve.

a scanning electron microscope (2007 Zeiss EVO60 at the AMNH).

**CT scanning.**—Two partial cranial specimens (*Gomphos* and the provisionally assigned arctostyloid) were CT scanned. Both specimens were scanned on a GE vltomelx s240 system at the AMNH. For the *Gomphos* specimen, voltage was 170 kV, current was 160  $\mu$ A, and exposure time was 750 ms. Voxel size was 0.0251 mm. Copper filter thickness was listed as “Unknown,” indicating that either no filter was used or the data were not entered. The parameters for the arctostyloid specimen were the same, except that the current was 170  $\mu$ A, a copper filter of thickness 0.5 mm was used, and voxel size was 0.0289 mm. Segmentation and volume rendering on both scans were performed in VGSTUDIO Max 3.5.1.

**Terminology.**—Terminology for Ostracoda follows that of Neustrueva et al. (2005). Terminology for mammalian teeth follows that of O’Leary et al. (2013; i.e., that the primitive condition for the four premolar loci for species in the clade Placentalia is identified as p1/P1, p2/P2, p4/P4, and p5/P5 [traditional p1/P1, p2/P2, p3/P3, p4/P4]).

**Repositories and institutional abbreviations.**—All newly described fossils are in the collections of the Paleontological Institute of the Mongolian Academy of Sciences, Ulaanbaatar, Mongolia. Casts of these specimens reside in the American Museum of Natural History, New York, New York, USA. Abbreviations are: American Museum of Natural History, New York, New York, USA (AMNH); Chernyshev’s Central Museum of Geological Exploration Saint Petersburg, Russia (CCMGE); Inner Mongolian Museum, Hohhot, China (IMM); Institute of Vertebrate Paleontology and Paleoanthropology, Beijing, China (IVPP); Mongolian Academy-American Museum Paleontological Expedition (MAE); Mongolian Paleontological Center-Mammal Collection, Academy of Sciences of Mongolia, Ulaanbaatar, Mongolia (MPC-M); Museum of Comparative Zoology, Harvard University, Cambridge, Massachusetts, USA (MCZ); Museo de Historia Natural “Alcide d’Orbigny,” Cochabamba, Bolivia (MHNC); Paleontological Institute of the Russian Academy of Sciences (PIN); Paleontological Institute, Mongolian Academy of Sciences, Ulaanbaatar, Mongolia (PIN MAS, PSS-MAE); Paleozoological Institute of the Polish Academy of Sciences,

Warsaw, Poland (Z. Pal.); Zoological Institute, Russian Academy of Sciences, Saint Petersburg (ZIN).

### Systematic paleontology

Ostracoda Latreille, 1806  
 Podocopida Müller, 1894  
 Cytheroidae Baird, 1850  
 Limnocytheridae Klie, 1938  
 Genus *Limnocythere* Brady, 1868

**Type species.**—*Limnocythere inopinata*, Baird, 1843.

*Limnocythere nemegtensis* Szczechura, 1971  
 Figure 4.1

**Type materials.**—Holotype: Z. Pal. No. MgO/25. Right valve. Paleogene, Naran Member (“White Beds”) of the Naran Bulak Formation, Gobi Desert, Mongolia.

**Diagnosis.**—“Carapace angularly-ovate in lateral outline, in front of the middle bearing a deep sulcus which is nodose anteriorly. Large, rib-like inflation occurs in anterior part of the carapace, extending adventrally below the sulcus turning upwards to disappear posteroventrally. Similar inflation runs below the posterodorsal margin. Valve surface strongly pitted” (Szczechura, 1971, p. 92).

**Occurrence.**—The type locality is in the Paleogene Naran Member (“White Beds”) of the Naran Bulak Formation, western Nemegt Basin, southwestern Mongolia at the localities Ulan Bulak, Tsagaan Khushu, and Naran Bulak (Szczechura, 1971). The new specimen described here is also from the Naran Member, Naran Bulak Formation, but from the central-eastern Nemegt Basin locality Daus-1. The species has been reported from the late Paleocene Bayanulanian Asian Land Mammal Age of the Nomogen Formation, Erlian Basin, Nei Mongol, China (Wang et al., 2019) and from three additional Paleocene deposits: the Subeng section, Inner Mongolia (Nei Mongolia), China, and the Xhinzuang and Shashi formations of China (Van Itterbeek et al., 2007).

**Description.**—The specimen has the diagnostic features of the type as follows: carapace small, angularly ovate in lateral



outline, dorsal margin almost straight, and ventral margin concave anteromedially and slightly rounded posteriorly. In the middle, at the dorsal margin, a transverse depression appears, extending to middle of carapace, and the depression expands to the dorsal margin. Conspicuous rib-like thickening extends along ventral margin of the carapace; and valve surface weakly pitted.

*Materials.*—N 5/69a PIN MAS, one complete carapace. Collected in 2014.

*Remarks.*—Brady (1868, p. 121) named the genus *Limnocythere* but did not provide a conventional species diagnosis writing only the species names “*L. inopinata* (Baird); *monstrifica* (Norman)” followed by notes on the morphology of their antennae. Meisch (2000, p. 427) later specified that *L. inopinata* is the type species. Brady (1868) remarked that extant members of this genus were found in the clay of bottom substrates.

The Naran Member of the Naran Bulak Formation has yielded numerous ostracode fossils (Khand, 1987). When describing Naran Bulak Formation ostracodes, Szczechura (1971, p. 87) wrote: “it is impossible to draw conclusions as to the age of the studied sediments on the basis of the ostracods.” Her basis for inferring a Paleocene age for *Limnocythere nemegtensis* was the context of geological work by Gradziński et al. (1969, p. 87), who stated that a Paleocene age could only be assigned “provisionally” to what is now considered the Naran Member of the Naran Bulak Formation. Szczechura (1971) wrote that the genus *Limnocythere* had been described as a Paleocene taxon citing “Morkhoven (1963)” (apparently an erroneous citation of Van Morkhoven, 1962, because the titles are identical). We could not, however, corroborate this age in Van Morkhoven (1963, v. II, p. 406–409) who described *Limnocythere* as Oligocene–Recent. *Limnocythere nemegtensis* appears to be endemic to Asia, known from both Mongolia and, more recently, from the Erlian Basin, Inner Mongolia, China, where the sediments yielding this ostracode have been dated using biostratigraphy, chronostratigraphy, and magnetostratigraphy as Paleocene Bayanulanian beds (Wang et al., 2019, p. 294–295). *Limnocythere* is a freshwater taxon (Van Morkhoven, 1963).

Cypridoidea Baird, 1845  
Cyprideidae Martin, 1940  
Genus and species indet.

#### Figure 4.2

*Occurrence.*—Locality Daus-1, Paleogene, Naran Member (“White Beds”) of the Naran Bulak Formation, Gobi Desert, Mongolia.

*Description.*—This taxon is known from a fragmentary valve that exhibits key morphological features distinguishing it from other taxa, including a rostrum-like process (beak adjacent to a groove and ridge) and a cyathus along the ventral margin of the left valve. The valve surface is strongly pitted.

*Materials.*—N 5/69b PIN MAS left valve, fragment, lower part of right valve of ostracode. Collected in 2014.

*Remarks.*—The morphological features noted above, as well as a distinct groove bordered by a ridge, and a cyathus are typical of the family Cyprideidae (Martin, 1940, 1958; Sames, 2011). The family, particularly the genus *Cypridea*, is a common element in nonmarine late Mesozoic to early Cenozoic faunas nearly worldwide (Sames, 2011). Despite having morphological features similar to those commonly described for *Cypridea*, N 5/69b PIN MAS is incomplete and damaged, making generic and specific assignment uncertain.

Mammalia Linnaeus, 1758

Eutheria Gill, 1872

Placentalia Owen, 1837

Pantodonta Cope, 1873

Pantolambdaoidea Cope, 1883

Pantolambdodontidae Granger and Gregory, 1934

Archaeolambdidae Flerov, 1952

Genus *Archaeolambda* Flerov, 1952

*Type species.*—*Archaeolambda planicanina* Flerov, 1952, p. 44, fig. 1, PIN 534-68, from “Paleocene of the Nemegt Basin, Gobi Desert,” Mongolia (Kielan-Jaworowska, 1968, p. 135) and by original description.

*Diagnosis.*—As given in Kielan-Jaworowska (1968, p. 135).

*Archaeolambda* cf. *A. planicanina* Flerov, 1952

#### Figure 5

*Type materials.*—Holotype: PIN 534-68, a mandible with left canine–m3 and right p1–m3 from the Paleogene beds of the Nemegt Basin, Mongolia, by original description. Simons (1960) synonymized the genus *Archaeolambda* with the previously named *Haplolambda*; however, we follow Kielan-Jaworowska (1968, p. 133–134) who subsequently identified features distinguishing the genera.

*Diagnosis.*—Specimens with the strongly crested, dilambdodont lower molars characteristic of Pantodonta, whereby the major cusps are connected by pronounced crests and trigonids are higher than talonids (Flerov, 1952; Simons, 1960; Kielan-Jaworowska, 1968). The lower dentition exhibits the diagnostic feature of the family Archaeolambdidae of “talonids in lower molars shorter and narrower than trigonids” (Kielan-Jaworowska, 1968, p. 135). Additionally, the specimen exhibits the diagnostic genus-level features of low and narrow molar talonids (Simons, 1960, p. 27).

*Occurrence.*—Holotype from the Paleogene beds of the Nemegt Basin, Mongolia (Flerov, 1952; Kielan-Jaworowska, 1968; Li and Ting, 1983); new lower dentition from locality Daus-1 and the new upper dentition from Daus-2b, both from the Paleogene Naran Member (“White Beds”) of the Naran Bulak Formation, central-eastern Nemegt Basin, Mongolia.

*Description.*—Both specimens, particularly the upper dentition (PSS-MAE 670), exhibit extensive postmortem damage. Although the lower dentition (PSS-MAE 662) appears slightly

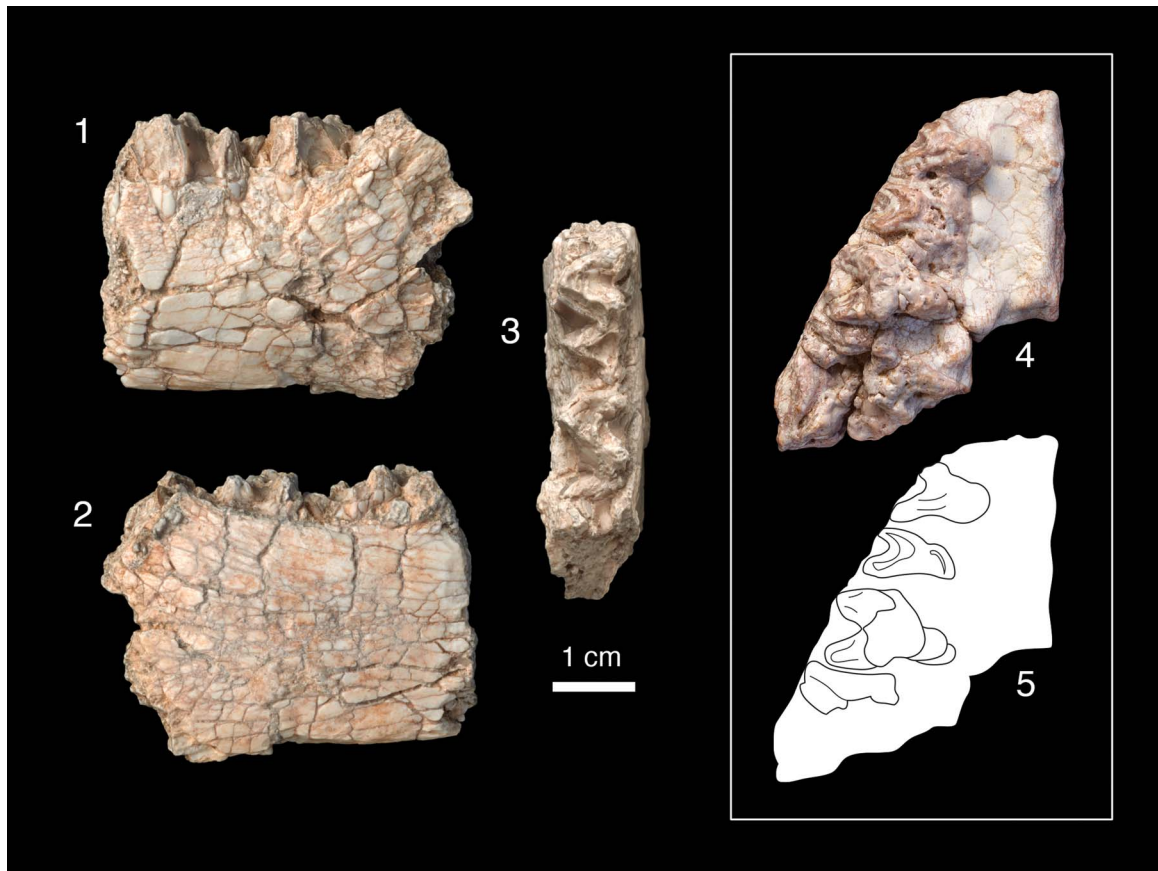


**Figure 5.** Dentitions of *Archaeolambda* cf. *A. planicanina*. Left dentary (PSS-MAE 662) with m2–m3 in (1) labial, (2) lingual, and (3) occlusal views; (4, 5) right maxilla (PSS-MAE 670) in occlusal view with drawing of the same showing P5–M2 and mesialmost labial root of M3.

larger, the sizes of the two specimens are similar enough that without better material (and because much of the comparative material consists of isolated lower and upper dentitions), the new specimens are tentatively referred to the same taxon.

The lower dentition consists of a left m2 and m3, with the base of the mandibular ramus preserved laterally adjacent to the talonid of m3. The m2 is fully intact but the m3 preserves only the trigonid. The new lower dentition is slightly larger than the holotype, which is a lower dentition of *Archaeolambda planicanina* figured in Flerov (1952, fig. 2) and examined on a cast of the same (AMNH 56621). Differences include that the length of the m2 of the new specimen, PSS-MAE 662, is closer in size to the length of the m3 of the holotype. The dentary under the trigonid of m2 is slightly deeper in the new specimen (holotype = 2.0 cm vs. PSS-MAE 662 = 2.6 cm). The talonid and trigonid of m2 are more open in the new specimen than they are in the cast of the holotype (AMNH 56621), the latter feature not being well represented, as illustrated in Flerov (1952, fig. 2).

On the upper dentition, postmortem weathering has exposed the tooth roots and removed the cusps, which eliminated many details necessary for synapomorphy-based taxonomic assignments and for assessment of full tooth dimensions. We tentatively also refer this maxilla to *Archaeolambda* cf. *A. planicanina* based on the tooth outline shape and overall dimensions of the teeth. On what we recognize as M2, the tooth outline forms an acute

triangle, suggesting the full tooth was limited to a paracone, metacone and protocone, also suggested by the pattern that the premolars and molars are each separated by a complementarily acute triangular space. The P5–M2 (traditional P4–M2) each had three roots (one lingual and two labial) and, judging by the position of the lingual root, the mesial-most two teeth are distinctly narrower in the labial-lingual dimension than either of the more distal teeth. This morphology and the overall tooth size have broad similarity to *Archaeolambda planicanina* (PIN 534-68, a P4–M1) figured in Flerov (1952, fig. 1) and examined on cast AMNH 56618, which shares two loci (P5 [traditional P4] and M1) in common with the new specimen, given our hypothesis of homology. Additionally, pairs of exposed labial roots of the M1–M2 and a small part of the mesial-most root of M3 are visible and the lingual edge of the protocone of M2 is convex. The M2 of the new specimen forms a very acute angle lingually, more so than does the M2 of *A. planicanina* described by Kielan-Jaworowska (1968). In this feature, the new M2 also resembles the holotype of *A. tabiensis* Huang, 1977 (IVPP 4333 and cast AMNH 126866). However, because of the poor preservation of the new specimen, no synapomorphic features can be identified with *A. tabiensis* and we do not refer it to that taxon here.

The morphology of the maxilla has also informed our tooth loci homologies. The well-preserved palatine process of the right maxilla has posterior and medial edges that are intact. The distal



edge exhibits a bony protrusion, similar to that reported by Kielan-Jaworowska (1968, fig. 1) for *Archaeolambda* cf. *A. planicanina* (Z. Pal. No. MgM-I1/54) directly lingual to M2. Neither sutures nor greater and lesser palatine foramina are preserved on the oral surface of the palatine process, but two small foramina can be seen on the posterior end of the palate.

**Materials.**—PSS-MAE 662, a poorly preserved left dentary with m2–m3, collected in 2017 from Daus-1, and PSS-MAE 670, a poorly preserved right maxilla with ?P5–M2 (traditional P4–M2) and the mesial-most labial root of M3, collected in 2019 from Daus-2b. These were compared with specimens AMNH 56618 and 56621, casts of the holotype, with an additional specimen of *Archaeolambda planicanina* (Flerov, 1952), with *A. tabiensis*, AMNH 126866 (cast of IVPP 4333), and with the literature (Flerov, 1952; Kielan-Jaworowska, 1968).

**Measurements.**—PSS-MAE 662, m2: maximum mesiodistal length (ML) = 16.5 mm; maximum labiolingual width (MW) = 11.7 mm; trigonid width = 11.7 mm; talonid width = 8.7 mm; m3: maximum length (ML) = 12.1 mm; maximum width (MW) = 9.3 mm. PSS-MAE 670, right P5: maximum length (ML) = 8.5 mm; maximum width (MW) = 10 mm (est.); right M2, maximum length (ML) = 10.8 mm, maximum width (MW) = 12.8 mm.

**Remarks.**—Mandibles from a Naran Bulak locality in the Nemegt Basin described by Flerov (1952) were attributed to a new family, genus, and species: Archaeolambdidae and *Archaeolambda planicanina*. Simons (1960) collapsed this family into the Barylambdidae and the genus into *Haplolambda*. These synonymies were not, however, followed by Kielan-Jaworowska (1968) who presented additional maxillary material of *Archaeolambda* cf. *A. planicanina* and identified features of the maxillary dentition that supported retaining the taxonomy of Flerov (1952). Because the material we present is inadequate to resolve taxonomic debates, we follow this more recent taxonomic interpretation.

*Archaeolambda*, which is not known outside Asia, has been extensively reported from the Naran Member (“White Beds”) of the Naran Bulak Formation as a taxon of the Gashatan or Gashatan-equivalent ALMA or older (Li and Ting, 1983; Dashzeveg, 1988; Dashzeveg and Russell, 1988; Lucas, 1998; Ting, 1998; Wang et al., 1998; Bowen et al., 2002). It is important to note that Dashzeveg (1988) also reported *Archaeolambda* from the Bumban Member of the Naran Bulak Formation, thus suggesting that the taxon has an Eocene range in the Bumbanian ALMA, potentially complicating its stratigraphic usefulness. In a recent review, Lopatin (2020) distinguished *A. planicanina* as a Paleocene Gashatan taxon, versus *A. bogdensis* (Dashzeveg, 1980) as a middle Eocene Arshantan taxon, thus species-level discrimination may be necessary for *Archaeolambda* to be a useful index taxon (see also Dashzeveg, 1982).

Genus *Pantolambdodon* Granger and Gregory, 1934

**Type species.**—*Pantolambdodon inermis* Granger and Gregory, 1934.

cf. *Pantolambdodon* sp. indet.

Figure 6

**Occurrence.**—The new specimen is from locality Daus-2b, Naran Member, Naran Bulak Formation and was collected in 2019. Previously described specimens come from the Bayan Ulan locality, Inner Mongolia, China (Paepen et al., 2021), and previously undescribed specimens come from the Ulan Shireh beds, Mongolia.

**Description.**—PSS-MAE 671 is a weathered right astragalus with exposed trabecular structure and a damaged ectal facet. The trochlea is relatively broad mediolaterally, comparable in width to the astragalus neck, although the lateral edge of the trochlea is weathered, potentially distorting the comparison. The trochlea is also gently grooved with edges that are not strongly skewed; the medial edge is directed ~10° from a parasagittal plane. Medial and lateral edges converge somewhat distally. The articular surface of the trochlea does not extend onto the neck. The medial side of the trochlea is flattened for articulation of the medial (tibial) malleolus and there is no medial fossa. What remains of the fibular facet on the lateral side is also flat. The astragalus foramen is absent. In posterior view, the medially flaring nature of the ectal facet is apparent. The neck of the astragalus, which is relatively aligned with the trochlea, is short, comparable in length to the length of the trochlea.

The head of the astragalus extends medially from the neck and articulates with the navicular, cuboid, and a third bone described below. The navicular facet occupies approximately one half of the size of the head; the outline of the facet is broadly oval, with the long axis running from dorsal and lateral to plantar and medial. The surface of the navicular facet is convex dorsally, transitioning to concave plantad. A distinct lip marks the plantar extreme of the navicular facet. This distinctive structure we term here the capitular lip of the astragalus. The cuboid facet occupies approximately one quarter of the astragalus head. Despite damage, it is apparent that this facet was convex, relatively broad dorsally, and that it tapered to a point at the plantar extreme.

On the medial side of the astragalus head is an additional, relatively large facet occupying approximately one fourth of the head, which appears to have been for a bone in the tarsus known as the “navicular hook” or the “tibiale” (Matthew, 1937, p. 165, 179), or the “medial tarsal bone” (Hildebrand, 1978). Although this Daus astragalus is weathered, it is clear that the orientation of the facet for the navicular hook is almost perpendicular to the navicular facet. The facet for the navicular hook is convex and connects to the navicular facet by a smaller, flatter facet that is weathered.

On the plantar surface, the sustentacular facet is an elongate oval that does not contact the astragalus head. The ectal facet is gently concave and poorly preserved at its proximal and lateral extremes. Part of the cuboid facet extends onto the plantar surface where it likely contacted the calcaneus. Plantar view also reveals the facet for the navicular hook meeting the facet for the navicular on the astragalus head.

**Materials.**—We made direct comparisons of PSS-MAE 671 to the following: AMNH 147008, a batch-catalogued sample of

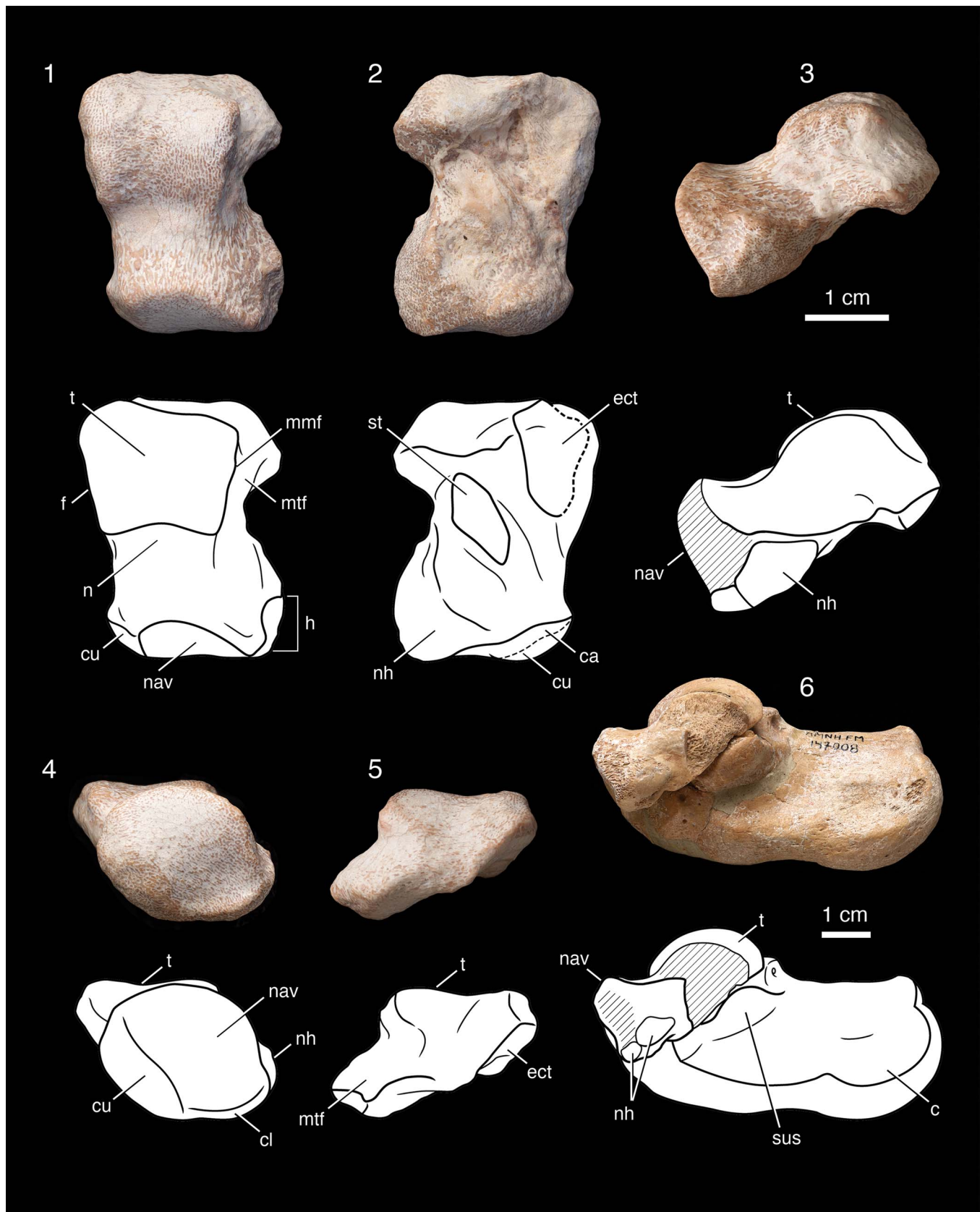


**Figure 6.** Tarsals of *Pantolambdaodon* sp. (1–5) PSS-MAE 671, a newly discovered right astragalus from the Naran Member of the Naran Bulak Formation, Mongolia, and (6), AMNH 147008, a right astragalus and calcaneus (not associated) collected in 1925 from the Ulan Shireh beds, Mongolia. Photographs with corresponding drawings beneath. Views are (1) dorsal; (2) plantar; (3) medial; (4) distal; (5) proximal; and (6) medial view of astragalus and calcaneus in articulation. c, calcaneus; ca, calcaneal facet; cl, capitular lip; cu, cuboid facet; ect, ectal facet; f, fibular facet; h, head; mmf, facet for the medial malleolus of tibia; mtf, medial tibial facet; n, neck; nav, navicular facet; nh, facet for the navicular hook; st, sustentacular facet; sus, sustentaculum tali; and t, trochlea.

tarsals that are not associated, including eight astragali, attributed to *?Pantolambdodon* from Eocene Irdin Manha beds of Inner Mongolia, China; AMNH 16663, *Pantolambda bathmodon* Cope, 1882; AMNH 81715, a collection of multiple astragali (not associated) of the perissodactyl *Lophialetes expeditus* Matthew and Granger, 1925; and AMNH 5021, the mesonychian *Mesonyx obtusidens* Cope, 1871. Additional comparisons were made in the literature to the astragalus *Pantolambdodon* sp. (IMM-1995-BAYU-070; Paepen et al., 2021) and to *Alcidedorbignya inopinata* (Baird, 1843) (MHNC 8372; de Muizon et al., 2015).

**Measurements.**—Maximum length of the astragalus = 33.6 mm; maximum width of the trochlea = 20.3 mm; maximum width of the head = 20.9 mm. Overall maximum width inestimable due to postmortem damage.

**Remarks.**—The new astragalus, PSS-MAE 671, compares closely with the astragalus recently described and figured as *Pantolambdodon* sp. from the late early-middle Eocene deposits of Bayan Ulan, Inner Mongolia, China (Paepen et al., 2021, fig. 4F:1–6). Importantly, those authors posited a faunal association between dental and tarsal specimens of *Pantolambdodon* sp. that assisted us in the identification of this isolated astragalus. Additionally, AMNH 147008, an unpublished, batch-catalogued collection of tarsals that includes eight astragali and a calcaneus collected by the 1925 Central Asiatic Expedition from the Eocene Irdin Manha beds of Inner Mongolia, China, and cataloged as *?Pantolambdodon* (collection note, E. Manning) also appears to represent the same taxon. The bones cataloged under AMNH 147008 are much less weathered than PSS-MAE 671 and served as an important comparative basis for identifying articular facets on the new specimen.

The calcaneus of AMNH 147008, although not necessarily associated with any of the astragali batch cataloged under the same number, was placed in approximate articulation with one of them. This exercise revealed that the third facet on the astragalus head did not articulate with the calcaneus and was likely for an absent bone, the navicular hook. Such a bone, which was reported in *Pantolambda bathmodon* from Paleocene (Torrejonian) rocks (Matthew, 1937), was described as articulating with both the astragalus and the body of the navicular. This additional tarsal also has been described in rodents as a medial tarsal bone serving as the site of attachment for the tibialis posterior muscle (Hildebrand, 1978). A similar facet was figured in the Paleocene pantodont from Bolivia *Alcidedorbignya inopinata* and termed the supplementary astragalocalcaneal facet (de Muizon et al., 2015, fig. 103; erroneously labeled as on the lateral side of the astragalus in fig. 102C.). However, as noted above in *Pantolambdodon* sp., it does not appear that this facet contacted the calcaneus. In both the Daus specimen PSS-MAE 671 and the *Pantolambdodon* specimens of AMNH 147008, the facet for the navicular hook has a small, distal extension that contacts the facet for the navicular on the head of the astragalus at the capitular lip.

Features in common among all of the specimens mentioned that are referred to *Pantolambdodon* sp. are similar overall size, relative shallowness of the trochlea, presence and proportions of

cuboid and navicular facets on the astragalus head, presence of a facet for the navicular hook, and lack of an astragalus foramen. They also share a distinctive crest on the plantar aspect of the navicular facet on the astragalus head (visible in Paepen et al., 2021, fig. 4F6), which we call the capitular lip of the astragalus and hypothesize may be a synapomorphy of *Pantolambdodon* sp. and close relatives. The capitular lip is absent in other taxa that have both a cuboid and a navicular facet on the astragalus head such as *Mesonyx obtusidens* (AMNH 5021; see also O’Leary and Rose, 1995) and is absent in other pantodonts such as *Pantolambda bathmodon* (AMNH 16663) and *Alcidedorbignya inopinata* (de Muizon et al., 2015, fig. 102). There is, however, a capitular lip on the astragalus of perissodactyls such as *Lophialetes expeditus* (AMNH 81715) and *Hyracotherium* (Kitts, 1956). Pantodonts have been considered part of the clade Ferae (McKenna and Bell, 1997; Paepen et al., 2021), and thus not particularly closely related to Perissodactyla. Thus, this shared resemblance is likely to be a homoplasy.

A difference between PSS-MAE 671 and both the AMNH specimens and the Paepen et al. (2021) specimen is that in PSS-MAE 671 the trochlea is more symmetrical. PSS-MAE 671 is also ~25% smaller than most of the other specimens (although one of the AMNH 147008 astragali is of comparable size), and appears to have had a slightly more elongate neck.

*Pantolambdodon* has been reported previously as an Eocene taxon from Arshatan and Irdinmanhan beds of Asia (Li et al., 2016; Paepen et al., 2021).

Glires Linnaeus, 1758

Mimotonidae Li, 1977

*Gomphos* Shevyreva, Chkhikvadze, and Zhegallo, 1975

**Type species.**—*Gomphos elkema* Shevyreva, Chkhikvadze, and Zhegallo, 1975.

**Other species.**—*Gomphos shevyrevae* Meng et al., 2009, and *Gomphos ellae* Kraatz, Badamgarav, and Bibi, 2009.

**Diagnosis.**—In part from Meng et al. (2004): similar to other mimotonids but differing from all other Glires in having two lower incisors. Differing from *Mimotona* in having a well-separated paracone and metacone and a distinct mesostyle on the upper molars. Differing from *Anatomylus* in having a shallow horizontal ramus (Averianov, 1994). Differing from *Mimolagus* in that *Gomphos* is of smaller size and has taller cheek teeth crowns with sharper cusps and ridges (Meng et al., 2004).

*Gomphos* cf. *G. elkema* Shevyreva, Chkhikvadze, and Zhegallo, 1975

Figures 7, 8

**Occurrence.**—The new specimen, collected in 2019, comes from locality Daus-2b, Naran Member (“White Beds”) of the Naran Bulak Formation, Paleogene of Mongolia. *Gomphos elkema* has been described from the Bumban Member of the Naran Bulak Formation in the region of Tsagan-Khushu, Nemegt Basin, Mongolia, beds that are considered lower Eocene (Shevyreva et al., 1975; Meng et al., 2004, p. 2), as



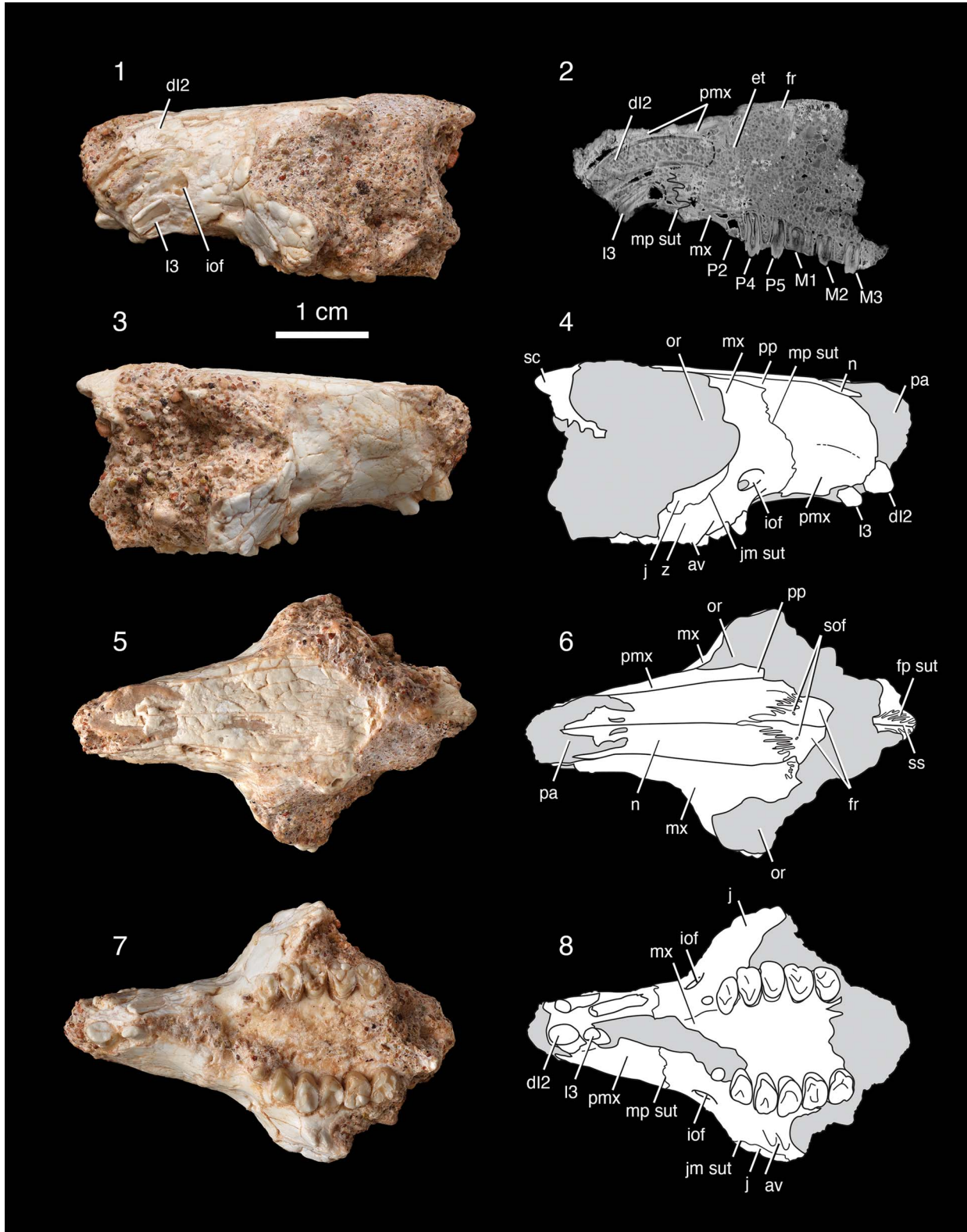


**Figure 7.** Skull of *Gomphos* cf. *G. elkema* (PSS-MAE 669). (1, 2) Left-lateral view and parasagittal CT scan slice showing left dl2 and I3 roots (dotted lines indicate distal ends of root; black line indicates maxillopalatine suture; note that the view of the dl2 root in 1 is shown from a slightly different position than it is in the CT slice in 2), and roots and crowns of P2, P4, P5, M1, M2, and M3; (3, 4) right-lateral view with the following teeth visible: dl2, I3, P2, P4, and P5; photograph and drawing; (5, 6) dorsal view, photograph and drawing; (7, 8) ventral view, photograph and drawing showing dl2 and I3 along with P2 (right side tooth; left side root), P4 and P5 and M1–M3. av, anteroventral zygomatic process of the maxilla; et, ethmoturbinal; fp sut, frontoparietal suture; fr, frontal; ioF, infraorbital foramen; j, jugal; jm sut, jugomaxillary suture; mp sut, maxillopremaxillary suture; mx, maxilla; n, nasal; or, orbit; pa, piriform aperture; pmx, premaxilla; pp, posterior process of the premaxilla; sc, sagittal crest; sof, supraorbital foramina; ss, sagittal suture; and z, zygomatic process of the maxilla.



**Figure 8.** Right upper post-incisor dentition of *Gomphos* cf. *G. elkema* (PSS-MAE 669) P2, P4, and P5, M1–M3.

well as the Gashato Formation, Ulan-Nur Basin of Mongolia (Dashzeveg, 1988; Dashzeveg and Russell, 1988; Asher et al., 2005). *Gomphos elkema* also has been reported from the Huheboerhe locality, Erlan Basin, Nei-Mongol (Inner Mongolia), where it has been used as an index taxon to identify the presence of Bumbanian-equivalent beds and the presence of a possible Paleocene-Eocene boundary section (Meng et al., 2004).

*Description.*—PSS-MAE 669 preserves a nearly complete, somewhat transversely compressed rostrum and a partial portion of the orbit and skull roof. The premaxilla is extensive and encloses the elongated curved roots of the upper incisors (homologized here as dI2 and I3, see comments below). The maxillopremaxillary suture is clearly demarcated on the right lateral side (but not on the left side) of the rostrum. This suture is finely interdigitated, which is a feature described in the gliroid *Rhombomylus* as characteristic of more mature individuals (Meng et al., 2003). A conspicuous posterior process of the premaxilla (Meng et al., 2003) flanks the nasal on the roof of the rostrum. The posterior terminus of this process is obscured by damage. Asher et al. (2005) specified a narrow anterior process of the frontal bone inserting between the premaxilla and the maxilla as a feature of *Gomphos elkema*, but this region is not preserved in the Daus specimen. The Daus specimen, however, does have a narrow anteriorly and broad posteriorly, V-shaped projection of the frontal bone between the nasals, which Asher et al. (2005) described as shared with leporids.

On the palate, the maxillopremaxillary suture is located in the large diastema between the distal upper incisor and P2. This intersection is well mesial to P2. In CT scans the position of the maxillopremaxillary suture relative to the tooth roots can be observed. The premaxilla encases most of the roots of the upper incisors. The root of dI2, but not that of I3, extends for a short distance into the maxilla. On the palate in the midline, the maxillopremaxillary suture is obscured by matrix. A CT scan reveals symmetrical scrolls of bone inside the posterior nasal cavity; these are interpreted as ethmoturbinals.

The roof of the nasal cavity is partially intact, and the nasal bones are prominent elements of the facial skeleton. At the front

of the snout the nasals are broken such that their lateral edges are poorly defined. Two oval openings, one in each nasal bone, are present near the midline. These openings may be foramina or products of breakage. The nasals project distinctly over the piriform aperture. The finely interdigitated frontonasal sutures indicate that the nasals extend posteriorly on the skull roof to the anterior margin of the orbit. The supraorbital foramina are minute, oval openings on the anterior aspect of the frontal, that are best preserved on the right side.

The maxilla in PSS-MAE 669 preserves the facial process, parts of the palatine, and parts of the zygomatic processes; the orbital process is obscured by matrix. The infraorbital foramen is visible on both sides, but is particularly clear on the right maxilla, where it opens above P2. A shallow trough extends forward several millimeters anteriorly from the foramen, but there are no other evident scars or muscular depressions on the face indicative of attachments for snout muscles. The zygomatic process of the maxilla is well developed and convex anteriorly. On the right side there is a partially preserved portion of the anteroventral zygomatic process of the maxilla as seen in *Rhombomylus* (Meng et al., 2003). A distinct jugomaxillary suture visible on the right side indicates that the jugal makes a substantial contribution to the anterior part of the zygoma. In ventral view, the root of the zygomatic process of the maxilla lies lateral to P5 and M1. The palatomaxillary suture is not visible and it is not clear whether it was absent or obscured by poor preservation. In PSS-MAE 669, a fragment of bone at the posterior aspect of the right orbit preserves the anterior part of the sagittal crest and the highly interdigitated suture between the right frontal and parietal. The sagittal crest is a low, blunt ridge.

Two enlarged upper incisors in the Daus specimen are preserved on the right side of the skull. Based on ontogenetic studies in rodents and lagomorphs (Luckett, 1985), the anterior incisor in *Gomphos* and other Glires has been homologized as dI2 (Li et al., 1987; Luckett and Hartenberger, 1993; Meng et al., 2003). Asher et al. (2005) observed that *Gomphos* resembles extant lagomorphs in having two pairs of upper incisors, whereas this more distal incisor is absent in many early Glires such as *Rhombomylus* (Meng et al., 2003) and rodents. The observation that the tooth at this locus undergoes replacement is the basis for its identification as I3 in adult lagomorph skulls

(Luckett, 1985), a state shared with *Gomphos* (Asher et al., 2005, fig. S10). The left incisor crowns are not preserved. The left premaxilla has been sheared off laterally, exposing the pulp cavities of the broken left incisor roots. As a result, the pulp cavities are filled with matrix, which improved their contrast and visibility in the CT scan. As noted above, dI2 is a robust tooth with a root that arcs through the premaxilla into the anterior maxilla where it terminates in a crypt. The right dI2 crown is largely missing, apparently worn down through use in life. There is an indication of enamel on its labial and mesial surfaces. dI2 is oval in occlusal outline. I3 is much smaller than dI2 (~25% of the area of dI2). The extent of enamel on the surface of I3 is obscured.

In PSS-MAE 669, the post-incisor dentition shows considerable wear and damage, but the crown features of the cheek teeth are preserved well enough on the right side of the skull to show diagnostic cusps, connecting ridges, and wear facets. The right P2 has a very slightly bicuspid crown in lingual profile. A shallow lingual wear facet extends posteriorly from the apex of the crown. The tooth has a broadly circular outline in occlusal view.

P4 (P3 of Meng et al., 2004) is oval in outline in occlusal view. Its lingual portion shows extensive wear and the protocone is preserved as a flattened ridge with continuous, well-worn mesial and distal lophs that extend labially. On the labial margin of the crown, a prominent, conical centrolabial cusp lies mesial and slightly lingual to an additional, less robust, distolabial cusp. A shallow triangular basin lies between the centrolabial cusp and the protocone. Deep within this basin is a low ridge connected to the mesial loph, and the apex of this ridge forms a weak conule. The hypocone and lingual and labial cingula are absent.

P5 (P4 of Meng et al., 2004) is oval in occlusal outline, but more transversely elongate than is P4. The apex of the protocone shows a distinct circular wear facet from which mesial and distal lophs extend. The centrolabial cusp is robust and a distolabial cusp is hardly discernable. A well-excavated, arcuate basin extends from the distolabial corner of the crown to the apex of the protocone; the basin is not evident on the anterior side of the tooth. As in P4, P5 lacks a hypocone and lingual and labial cingula.

The upper molars are more rectangular and less labiolingually transverse in occlusal view than P4 and P5. The right M1 is considerably worn, but its lingual profile suggests the presence of a hypocone in addition to a protocone. A prominent, swollen mesial loph extends from the protocone to the mesiolingual base of what was likely the paracone; only the cusp is broken. The posterior protocone loph is more crest-like and extends to the distolingual base of the metacone. The metacone is not as prominent as the paracone, but both cusps are considerably worn. The metacone is slightly more lingual than the paracone, giving the labial margin of the crown an oblique outline that trends mesiolabial to distolingual. The most distinctive feature of M1 is a broad and deeply excavated trigon basin rimmed by the surrounding cusps and lophs. A metaconule is either absent or obscured by wear. The styler region of the tooth is poorly preserved.

M2 is similar to M1 in its occlusal outline and many other features. M2 also differs from M1 in lacking a deeply excavated

trigon basin. M2 has a distinctly robust paracone and metacone. The presence of a mesostyle is ambiguous on M1 due to wear, however, the mesostyle is clearly present on M2. A narrow trough extends from the labial margin of the crown between the paracone and mesostyle to the center of the shallow trigon basin.

M3 shows well-defined wear facets at the apices of the paracone and metacone that extend lingually to become confluent with the wear facets of the protocone and its lophs. A distinctive feature of M3 is a small, but well-defined hypocone separated from the distal face of the protocone by a narrow trough. The worn apex of the hypocone is confluent with a postcingulum that extends to a crest descending from the metacone. Accordingly, the hypoconal postcingulum is clearly distinct from the higher distal loph of the protocone.

**Materials.**—PSS-MAE 669, an anterior skull preserving right and left maxillae, nasals, left anterior jugal, anterior infraorbital foramina, base of crowns of right dI2, I3, anterior roots of left dI2–I3, right P2, alveolus of left P2, right and left P4–5, M1–3. Comparisons were made with published illustrations as follows: upper teeth of *Gomphos elkema*, P3–M1 (IVPP-V13509.5), P5 (traditional P4)–M1 (IVPP-VI13509.6), P5 (traditional P4)–M2 (IVPP VI1509.4) from Meng et al. (2004, figs. 3, 4); upper cheek teeth of *Gomphos shevyreva*, V14669, V14671.1–V14671.4 from Meng et al. (2009, fig. 2); left upper dentition of *Mimotona wana* Li, 1977, with P4 (traditional P3)–M3, V4324 in Li (1977, fig. 2, pl. II 1a, b); upper teeth of *Gomphos ellae*, maxilla with M1–2 MPC 30/1 in Kraatz et al. (2009, fig. 4); and upper teeth of *Anatomylylus rozhdzhevskii* Averianov, 1974, labial fragment of right M1 (ZIN 9161) in Averianov (1994, fig. 4 K, L) (the right M1 is denoted as a left M1 in the text [Averianov, 1994, p. 404], but appears to be a right M1 in fig. 4) and right M3 (ZIN 9162, Averianov, 1994, p. 404; not illustrated).

**Measurements.**—PSS-MAE 669, all measurements of right dentition. P4 (P3 of Meng et al., 2004), maximum mesiodistal length (ML) = 2.5 mm, maximum labiolingual width (MW) = 4.2 mm; P5 (P4 of Meng et al., 2004), ML = 2.7 mm, MW (est.) = 5.0 mm; M1, ML = 2.9 mm, MW = 4.8 mm; M2, ML = 2.8 mm, MW = 4.2 mm; M3, ML = 3.2 mm, MW = 3.6 mm.

**Remarks.**—PSS-MAE 669 from Daus-2b closely resembles specimens of *Gomphos elkema*, a taxon named by Shevyreva et al. (1975) and described extensively based on new material by Meng et al. (2004). The species is known to occur in the upper beds of the “Nomogen Formation,” the Bumban Member of the Naran Bulak Formation, and members II and III of the Gashato Formation (Dashzeveg, 1988; Dashzeveg and Russell, 1988). Faunas from the Bumban Member generally have been recognized as early Eocene (Dashzeveg, 1982, 1988; Dashzeveg and Russell, 1988; Bowen et al., 2002; Meng et al., 2004), although some authors have considered them to be late Paleocene (Beard, 1998). Some features of the skull, dentition, and postcranial skeleton of *G. elkema* were briefly described by Asher et al. (2005), who also published a phylogenetic analysis of the taxon and other



selected Glires, non-gliroid eutherians, and marsupials. A few features of the skull are described here for the first time.

Other species in the genus also have been assigned to the Eocene. A new species, *Gomphos shevyreva*, was named and described from the middle Eocene lower beds of the Irđin Manha Formation in the Erlian Basin (Meng et al., 2009). A third species, *G. ellae*, was described from the middle Eocene Kholboldchi Formation at Tsagan Khutal, Mongolia (Kraatz et al., 2009). *Gomphos ellae* has been recognized as one of the youngest known mimotonids and the youngest species of *Gomphos* (Meng et al., 2009). In addition, a mimotonid genus, *Anatomylyus*, was described from the locality Andarak 2 in the lower part of the Alay beds, Kyrgyzstan, and proposed to have close similarities to *Gomphos* (Averianov, 1994). The Alay beds are considered early or middle Eocene (Averianov, 1994).

Comparisons between the Daus specimen, PSS-MAE 669, and the above listed taxa, underscore its close similarity and favored assignment to *Gomphos elkema*. *Gomphos shevyreva* has upper molars with more inflated and posteriorly expanded hypocones and lingual cingula. The widths of the cheek teeth of PSS-MAE 669 are more closely similar to those of *G. elkema* than to *G. shevyreva* (compare measurements herein with Meng et al., 2004, table 1; Meng et al., 2009, table 1). *Gomphos shevyreva* was diagnosed as having more robust teeth than *G. elkema*, but the measurements of the upper teeth of the latter reported by Meng et al. (2004) are actually greater than those given for *G. shevyreva* (Meng et al., 2009).

The third species of *Gomphos*, *G. ellae*, is represented by a single specimen, a lower jaw with a nearly complete dentition and an associated maxillary fragment with a heavily worn M1 and M2 (Kraatz et al., 2009). *Gomphos ellae* was only distinguished diagnostically from *G. elkema* by its deeper ramus, and distinguished from all other mimotonids, including other species of *Gomphos*, in having a proportionately longer diastema. Unlike the Daus specimen and *G. elkema*, the M1 and M2 referred to *G. ellae* do not show evidence of a well-developed hypocone, but upper molars in *G. ellae* are so heavily worn that this distinction is tentative.

*Anatomylyus* is another mimotonid taxon primarily distinguished by its short, robust, and deep jaw (see diagnosis above and Averianov, 1994). Only an incomplete M1 and a badly worn M3 in *A. rozhdestvenskii* can be compared with the Daus specimen. In contrast to the latter and *Gomphos elkema*, the M1 mesostyle in *A. rozhdestvenskii* is minute and the large postcingulum of M3 occupies almost half the crown.

Some gliroids (e.g., *Rhombomylyus*) have well-documented skull morphology (Meng et al., 2003). Notwithstanding the brief description of *Gomphos* in Asher et al. (2005), there has not been a detailed monographic treatment of the cranial osteology of *Gomphos*. One emerging difference between *Gomphos* and *Rhombomylyus* that invites further examination is the morphology of the nasal bones, which may be pierced by foramina in *Gomphos* but are not in *Rhombomylyus* (Meng et al., 2003, fig. 23).

All previously described taxa of *Gomphos* are thus from Bumbanian-aged faunas generally assigned to the early Eocene or from younger faunas in Mongolia and the Erlian Basin of

China that are assigned to the middle Eocene (Shevyreva et al., 1975; Meng et al., 2004, 2005, 2009; Kraatz et al., 2009). The only mimotonid of the earlier Gashatan ALMA is the genus *Mimotona* (Li, 1977; Dashzeveg and Russell, 1988). The Daus specimen, however, is clearly referable to *Gomphos*, and not *Mimotona*, and more specifically to *G. elkema*, in having less-transverse cheek teeth, a clearly separated paracone and metacone, and a distinct mesostyle on the upper molars.

Arctostylopida Cifelli, Schaff, and McKenna, 1989

Arctostylopidae Schlosser, 1923

Genus and species indet.

Figures 9–12

*Occurrence*.—Locality Daus-2b, Naran Member (“White Beds”) of the Naran Bulak Formation, Mongolia. Collected in 2019.

*Description*.—The anterior cranium of PSS-MAE 673 shows surface bone only on the left side. In lateral view, the skull has a relatively short rostrum and a tall skull roof above the orbit. The face, particularly the anterior rostrum and the piriform aperture, has been elucidated with CT scans. The nasal bones are not preserved, but the position of what was the frontonasal suture appears largely intact. The anterior ends of the frontal bones protruded in the midline with the left and right sides meeting at a delicate point. The superior aspect of the piriform aperture is slightly recessed. The infraorbital foramen can be identified on the left side of the skull. Maxillopremaxillary sutures are not visible. In ventral view, the palate contains a large anterior opening, but it is not clear whether this was two separate incisive foramina or a single large opening. CT images show that choanae are preserved and the posterior edge of the palate is heart-shaped (posteriorly concave with a midline point), and that the posterior edges of the palatine were marked by a thickened rim known as a palatine torus. Interesting but more rarely described features of fossil mammal skulls, such as the sphenoid sinus, the basisphenoid, and a pterygoid process, also can be discerned in cross-sectional CT images of PSS-MAE 673.

The dentition is best preserved on the left side of the skull, but the right side was elucidated using a CT scan. The teeth are highly damaged and may also have been worn. Additionally, postmortem damage has resulted in a skewed relationship between the left and right sides of the dentition such that homologous alveoli are not aligned mediolaterally. Nonetheless either alveoli, roots, or partial teeth at each locus are preserved on each side.

In general, the specimen preserves tooth loci as roots at the junction of the crown. There is some distortion of the skull due to damage, and the right dentition is shifted slightly mesial to the left dentition. For reasons given below, we provisionally identify the most mesial alveoli on the right and left side as I3. Just distal to I3 are alveoli that we identify as those for the upper canines. The left I3 and C appear buccolingually compressed. Both have very worn crowns and there is no diastema between them. The CT scan shows that the pulp cavities of these teeth are exposed laterally, so the apparent buccolingual

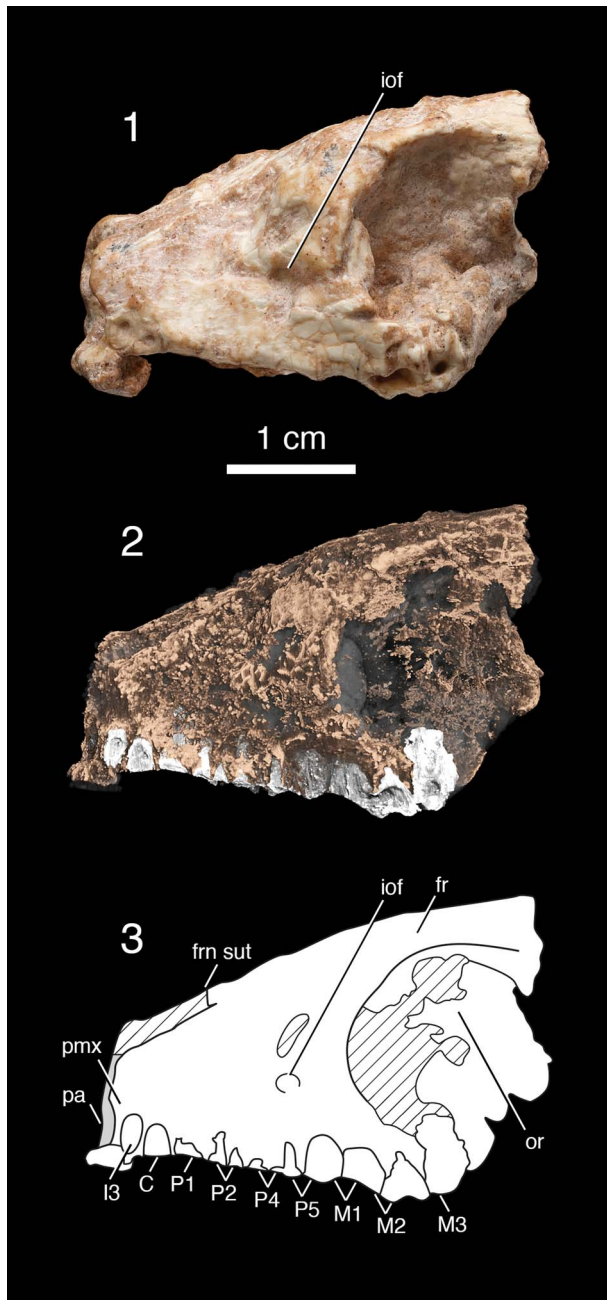


**Figure 9.** Skull of an arctostylopid, genus and species indet (PSS-MAE 673) in lateral view. (1) Digital photograph; (2) CT rendering; and (3) composite drawing. fr, frontal; frn sut, frontonasal suture (nasals not preserved); iof, infra-orbital foramen; or, orbit; pa, piriform aperture (opening preserved in part); pmx, premaxilla, and tooth loci (I3, C, P1–P5, M1–M3) are indicated. In the CT rendering, roots of some adjacent premolars and molars overlap in lateral view. Note the absence of a diastema. Striped areas are not preserved.

compression can be explained by breakage or erosion. What appears to be a root for the right I3 is rounder than the locus for I3 on the left. Additionally, the right root for I3 has an intact exterior surface that is surrounded by alveolar bone. Therefore, the right side is likely more informative about the incisor morphology.

There is no diastema between the canine and the succeeding postcanine tooth. Distal to the canine, a tooth root as it meets the crown base exists for what we hypothesize to be the P1, which

has a rounded base and is not markedly large relative to the adjacent teeth. Both C and P1 are single-rooted. Despite this uncertainty in the identity of the most mesial alveoli, the homologies of the more distal teeth are less ambiguous, and we identify these as P2, P4 (traditional P3), P5 (traditional P4), M1, M2, M3. P2 is two-rooted, P4 has two distinct roots and an incipient third root, and P5–M3 are three-rooted. P2 is mesiodistally elongate and transversely narrow. P4 and P5 are preserved only as the bases of the tooth crowns, which are roughly triangular in occlusal outline. M1 and M2 are quadrate in occlusal outline. Only the left M2 preserves some features of the molar crown, a lingual moiety with a prominent conical protocone. Distal and slightly labial to the protocone is a distinct sulcus bordered distally by a slight rise that appears to be part of a hypocone. Although the distolingual corner of the crown is heavily worn and damaged, it is extensive, suggesting that the hypocone was well developed. A distinct lingual cingulum extends distally from the base of the protocone. The surface of the cingulum is marked by a wear facet and crenulations that may be two or three tiny cusps. M3 is only preserved as a deeply worn base of the crowns and roots; the CT scan shows evidence of a highly worn protocone. The outlines of the premolars and molars as indicated by the roots show labial indentations, but the labial crowns are not preserved, and it cannot be determined whether an ectoflexus, or other aspects of this region of the crowns, was present or absent.

**Materials.**—PSS-MAE 673, partial skull with worn and damaged crowns and tooth roots with partial crown of left M2. Compared directly with the following specimens and literature: *Palaeostylops iturus*, paratype AMNH 20415, left maxilla with partial C, P1, P2, P4, P5, M1–3 described by Matthew et al. (1929, fig. 2); AMNH 22143, left maxilla with I1–3, C, P1, P2, P4, P5, M1–3 described by Matthew et al. (1929, fig. 13); AMNH 21743, left maxilla and upper cheek teeth, numerous specimens from the PIN collections described and figured by Kondrashov and Lucas (2004, fig. 2); a large sample of *Palaeostylops iturus* in AMNH collections from the Gashato beds, Mongolia; *Palaeostylops macrodon* (Matthew, Granger, and Simpson, 1929), AMNH paratype 22144, left maxilla with P2, P4, P5, M1–3, right maxilla with M1–3 described by Matthew et al. (1929, figs. 11, 12); a large sample of *P. iturus* and *P. macrodon* from the Gashat locality in the MPC-M collections figured, measured, and statistically analyzed by Missiaen et al. (2012, fig. 2, table 1); *Arctostylops steini* Matthew, 1915, AMNH cast of MCZ 20004, anterior skull and associated mandible with nearly complete dentition described and figured by Cifelli et al. (1989, fig. 2); *Allostylops periconatus* Zheng, 1979, AMNH cast of IVPP 5043, type, anterior skull with well-preserved P2, P4, P5, M1–3 described by Zheng (1979) from the Chijiang Basin, China; *Asiostylops spanios* Zheng, 1979, AMNH cast of IVPP 5042, holotype, skull and mandibles with premolars and molars described by Zheng (1979); *Anatolostylops dubius* Zhai, 1978, AMNH cast of IVPP 4357, holotype, left M2–3 described by Zhai (1978, fig. 8); *Anatolostylops zhaii* Wang et al., 2008, IVPP 14657, holotype, and figured by Wang et al. (2008); *Enantiostylops* (*Sinostylops*) *progressus* (Tang and Yan, 1976), AMNH cast of IVPP 4264, right maxillary

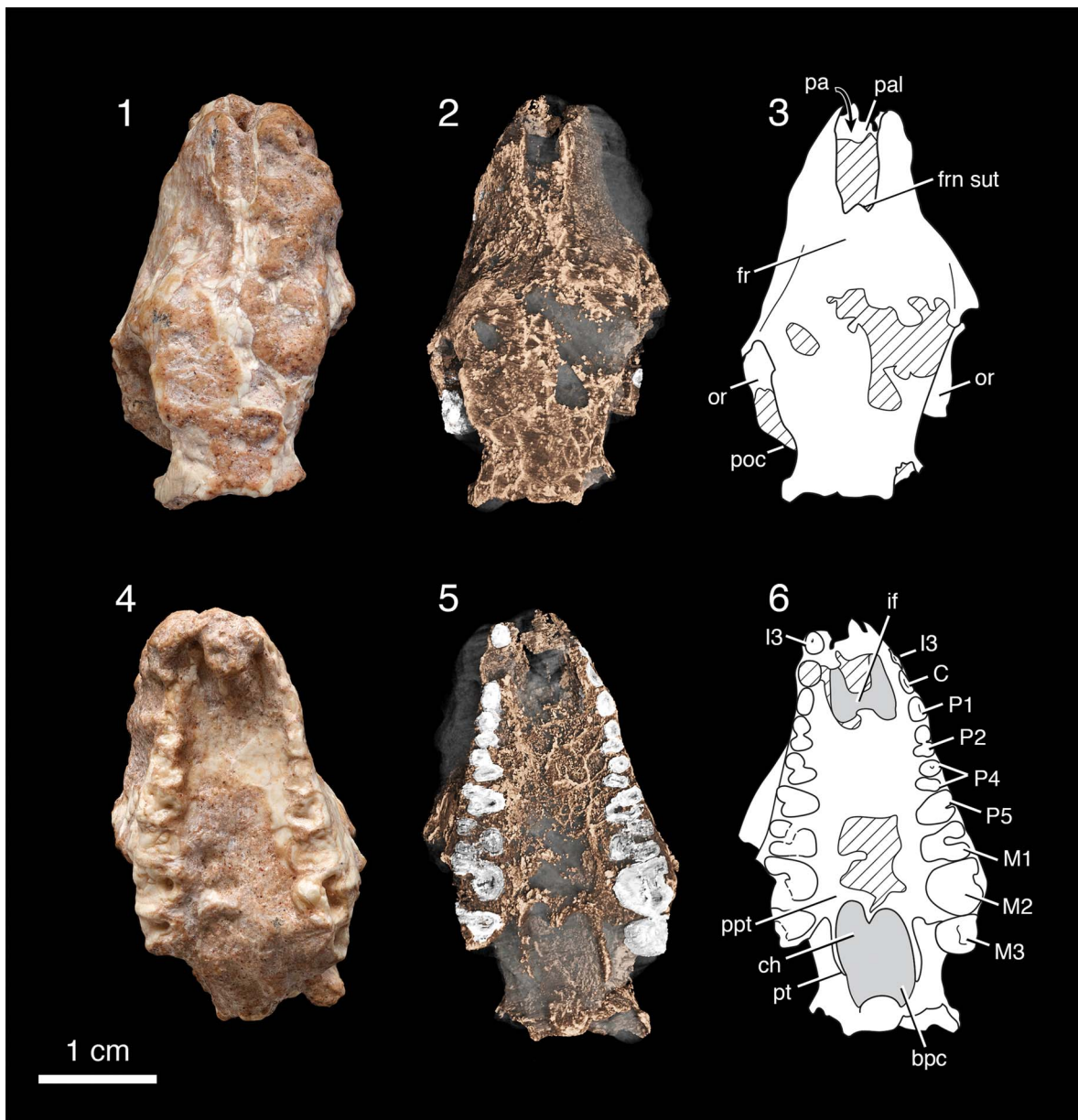


**Figure 10.** Skull of an arctostylopid, genus and species indet (PSS-MAE 673) (1–3) in dorsal views: digital photograph, CT rendering, and composite drawing; and (4–6) in ventral views: digital photograph, CT rendering, and composite drawing; tooth loci (I3, C, P1, P2, P4, P5, M1–M3) indicated on (6). bpc, basipharyngeal canal; ch, choanae; fr, frontal; frn sut, frontonasal suture; if, incisive foramen or foramina (may be one or two foramina); or, orbit; pa, piriform aperture (nasal bones that would have been at its superior aspect are not preserved); pal, hard palate; poc, postorbital constriction; ppt, postpalatine torus; pt, pterygoid process.

fragment with M1–3, described by Tang and Yan (1976) as *Sinostylops progressus*, erected as *Enantiostylops progressus* by Averianov (2020, appendix 1); *Kazachostylops occidentalis* Nesso, 1987, CCMGE 12/12455, right maxillary fragment with P4–5, M1–2 described and figured by Averianov (2020, fig. 2); *Migrostylops rosella* Tong and Wang, 2006, IVPP V10734: left I1–M3 described by Tong and Wang (2006, fig. 7.4; see also Missiaen et al., 2012, fig. 7.4).

Comparisons were also made with *Hyopsodus orientalis* Dashzeveg, 1977, described by Dashzeveg (1977, figs. 3–8) from the base of the Bumban Member of the Naran Bulak Formation at the Tsagan Khushu locality, Mongolia, and various upper dentitions of *Hyopsodus* from the early Tertiary of

North America, including *Hyopsodus paulus* Leidy, 1870, AMNH 10974, anterior skull with right cheek tooth dentition, and *Hyopsodus despiciens* Matthew, 1909, AMNH 11877, holotype, skull and jaws with nearly complete dentition described by Matthew (1909, figs. 103–105).

Comparisons were also made with various early perissodactyls: casts of *Rhodopagus pygmaeus* Radinsky, 1965 (AMNH 21554); figures and descriptions of *Rhodopagus* (Radinsky, 1965), *Pataecops minutissimus* (Reshetov, 1979) (Averianov and Godinot, 2005), *Yimengia* (Wang, 1988; Bai et al., 2020; Paepen et al., 2021), *Pataecops parvus* Radinsky, 1965, and *Minchenolestes erlianensis* Wang et al., 2011.



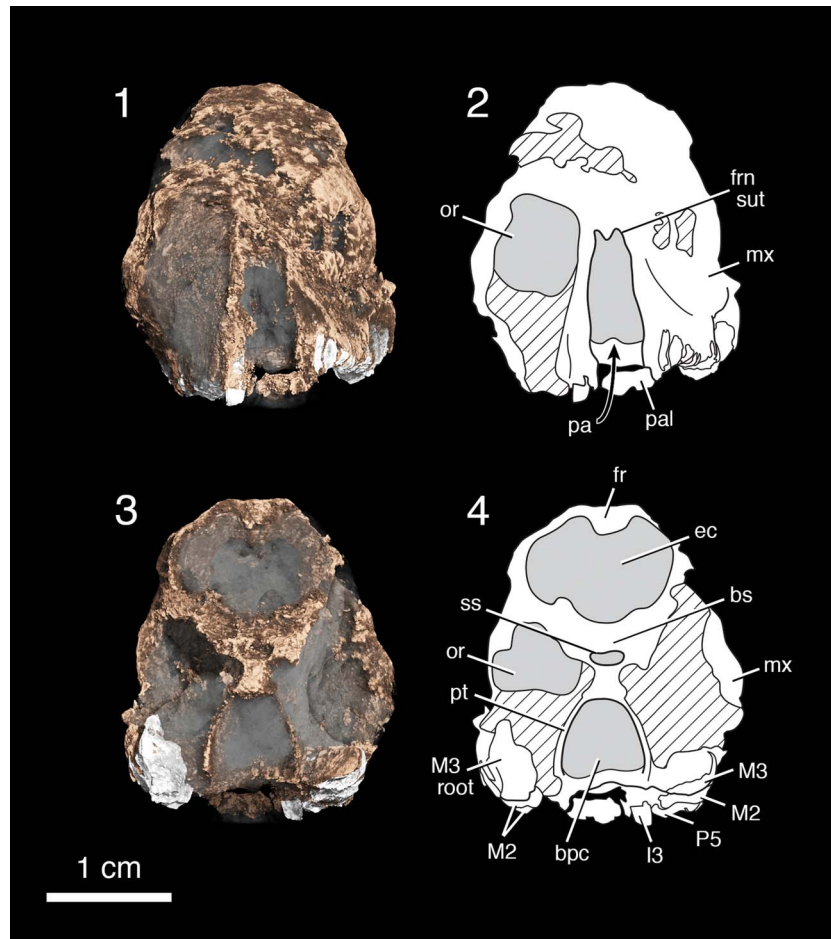


**Figure 11.** CT renderings and drawings of the skull of an arctostylopid genus and species indet (PSS-MAE 673) in (1, 2) anterior view and (3, 4) posterior view; tooth loci (I3, P5, M2, M3, M3 root) indicated on (4). bpc, basipharyngeal canal; bs, basisphenoid; ec, endocranial cavity; fr, frontal; frn sut, frontonasal suture; mx, maxilla; or, orbit (dimensions of orbit are approximated); pa, piriform aperture; pal, hard palate; pt, pterygoid process; ss, sphenoid sinus.

**Measurements.**—All measurements of left upper tooth loci. We note that, with the exception of M2, the teeth are preserved only at the junction of the root and crown; thus, these dimensions are approximate. P2: maximum mesiodistal length (ML) = 3.25 mm, maximum labiolingual width (MW) = 1.5 mm; P4 (traditional P3), ML = 3.10 mm, MW = 2.25 mm; P5 (traditional P4) ML = 3.2 mm, MW = 4.1 mm; M1, ML = 3.5 mm, MW = 4.5 mm; M2, ML = 5 mm, MW = 5 mm; M3, ML = 3.5 mm, MW = 4.25 mm.

**Remarks.**—This poorly preserved, enigmatic specimen from Daus-2b is so lacking in well-preserved dental features that its definite identification and allocation are precluded. Yet we argue here, based on comparisons of various taxa known from the Asian Paleocene and Eocene, that it has features most like those of arctostylopid. As in the diagnosis for Arctostylopidae (Cifelli et al., 1989, p. 5), the Daus specimen lacks any evidence of a diastema, a feature typical of early perissodactyls compared here, such as the ceratomorphs that are common to Eocene faunas in Mongolia and Asia. Another potential similarity to arctostylopid relates to the number of teeth. In arctostylopid the dentition is complete or nearly complete, with the number of upper incisors varying from three (e.g.,

*Palaeostylops iturus*, see Matthew et al., 1929, p. 12, fig. 13; *Migostylops rosella* Tong and Wang, 2006) to two (e.g., *Arctostylops steini*, see Cifelli et al., 1989, p. 8). Counting forward from M3 in the Daus specimen indicates the presence of a complete series between P1 and M3 and suggests that the three most-mesial alveoli are those for I3, C, and P1, in alignment with the condition in *A. steini*. There is enough damage at the anterior end of the rostrum to suggest that at least an I2 may have been lost in preservation. Also, in correspondence with the diagnosis of arctostylopid (Cifelli et al., 1989), the alveoli in the Daus specimen indicate that the upper canine is subequal in dimensions to the I3 and P1.

Unfortunately, the presence of the most striking feature of the arctostylopid upper dentition—the salient, straight ectoloph on the upper molars—cannot be ascertained in the Daus specimen because all the crowns of the latter, with the exception of the lingual moiety of M2, are either heavily worn to their roots or destroyed. Nevertheless, a number of features of the dentition and skull bear strong resemblance to various arctostylopid. Based on the dimensions and outlines of the base of the crowns and the roots preserved, the M2 is notably larger and more quadrate than M1, a feature very characteristic of *Palaeostylops* (Matthew and Granger, 1925; Matthew et al.,

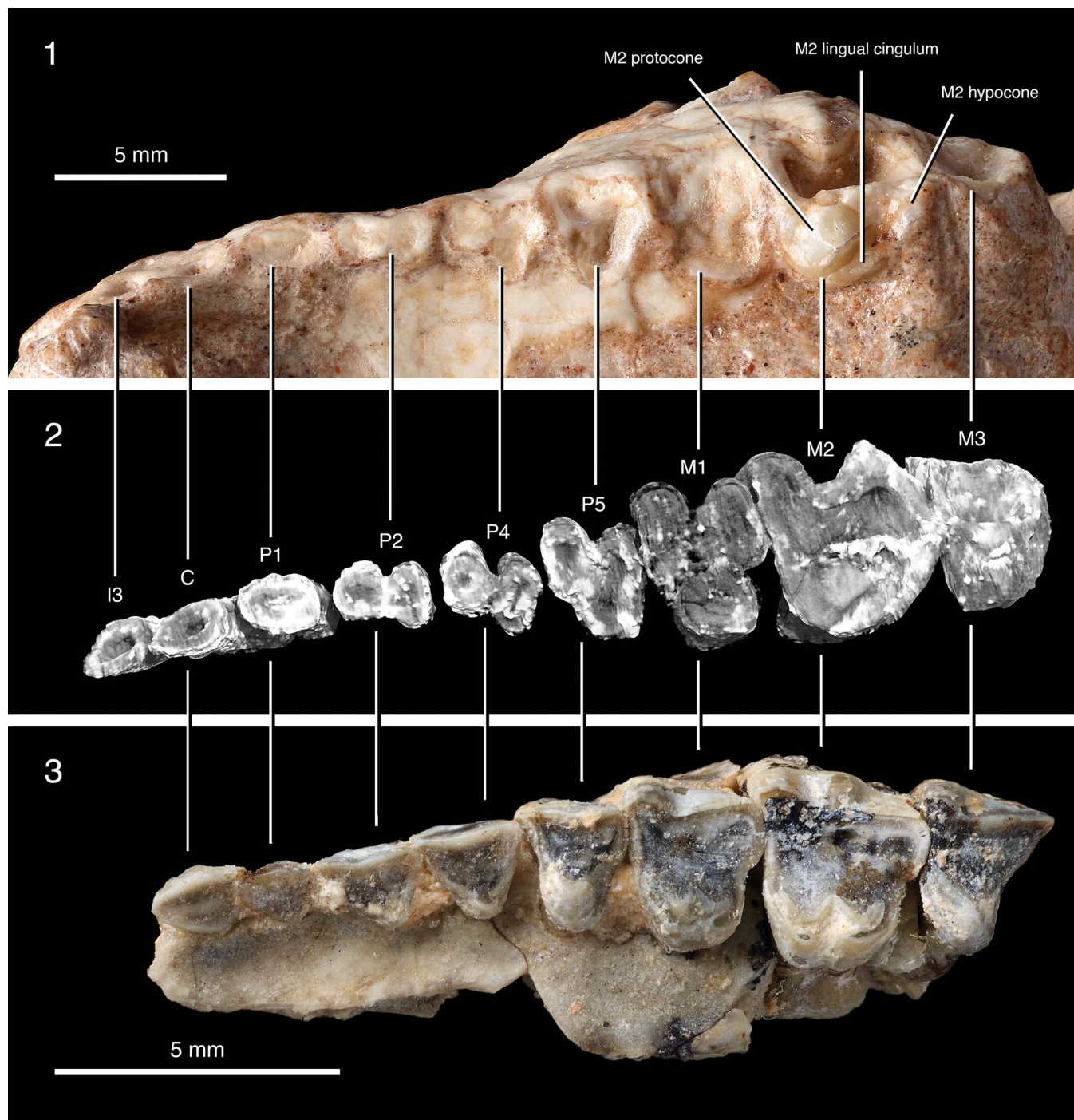


**Figure 12.** Left upper dentition of an arctostylopid, genus and species indet (PSS-MAE 673) with tooth loci (I3, C, P1–P5, M1–M3) indicated. (1) Digital photograph, (2) CT rendering, and (3) comparison with the upper dentition of *Palaeostylops iturus*, AMNH 21743. No tooth crown is fully preserved in PSS-MAE 673.

1929; Kondrashov and Lucas, 2004), *Arctostylops* (Matthew, 1915; Cifelli et al., 1989), *Anatolestylops* (Wang et al., 2008), and other taxa. This feature strongly differs from that seen early condylarths, including *Hyopsodus orientalis* from the Bumbanian of Mongolia (Dashzeveg, 1977), as well as early Asian perissodactyls (Radinsky, 1965; Wang, 1988; Averianov and Godinot, 2005; Wang et al., 2011; Bai et al., 2020; Paepen et al., 2021) where the M1 and M2 do not differ so greatly in basal dimensions. Although M3 is badly damaged in the Daus

specimen, it does appear notably smaller in overall dimensions than M2, a feature also characteristic of *Palaeostylops*, *Arctostylops*, and *Anatolestylops* (Cifelli et al., 1989, fig. 8). Other features of PSS-MAE 673 that are found in arctostyloids, including *Palaeostylops iturus*, are a P1 that is single-rooted and laterally compressed, P4, P5 with three roots, P4 base triangular in shape, M2 with a well-developed sulcus distal to the protocone, and a lingual cingulum with two or three small cusps (see Kondrashov and Lucas, 2004, p. 197–199). The expanded distolingual

corner of the crown in M2 also suggests that a well-developed but heavily worn hypocone is present. Comparison with a cast of *Arctostylops steini* (MCZ 20004) shows that this species has a heart-shaped posterior margin of the palate with a well-developed palatine torus that closely resembles the condition in the Daus specimen.

Obviously, the preservation in PSS-MAE 673 does not allow very resolved identification, but the features of the lingual moiety of M2, the only partially preserved aspect of the crowns of the teeth, can be compared with those of described arctostyloids. The lingual cingulum and the suggestion of a well-developed hypocone compare closely with the condition in *Palaeostylops iturus* (Matthew and Granger, 1925; Kondrashov and Lucas, 2004, fig. 2) and *P. macrodon* (Matthew et al., 1929, fig. 12). It is of interest that Cifelli et al. (1989) elevated the latter species to a new genus, *Gashatostylops macrodon*, which is diagnosed by the presence of the relatively larger upper and lower second molars, larger incisors, cuspules on the lingual cingula, absence of a sulcus between the protocone and hypocone, two rather than three incisors, and a laterally constricted snout. Based on a large sample of *Palaeostylops iturus* from the Gashatan horizon at Tsagan Khushu in the PIN collections, Kondrashov and Lucas (2004) found that nearly all the distinctive characters of *Gashatostylops* were either within the range of variation for specimens of *P. iturus* or could not be identified with certainty (e.g., the number of incisors) given the incomplete preservation in the cited specimens. In agreement with Kondrashov and Lucas (2004) and Missiaen et al. (2012), we recognize the original designation of Matthew et al. (1929) of *P. macrodon*.

As in *Palaeostylops*, the lingual region of M2 in *Arctostylops* shows a well-developed hypocone, but the lingual cingulum extends without interruption from the mesial face of the protocone to the distal face of the hypocone (Cifelli et al., 1989, figs. 2, 8). In contrast to these genera, *Asiostylops spanios* Zheng, 1979, from the late Paleocene of China (Li and Ting, 1983), either lacks a hypocone, or the hypocone is represented by a small cusp at the lingual terminus of a broad postcingulum. *Kazachostylops occidentalis* from the late Paleocene of Kazakhstan also lacks a hypocone on the upper molars, but has both pre- and postcingula that are non-continuous (Nessov, 1987; Averianov, 2020). *Anatostylops dubius* and *A. zhaii* from the early Eocene of China are distinctive in having a protocone and hypocone placed well labially and forming a continuous ridge separated by a deep fossette from the ectoloph (Zhai, 1978; Wang et al., 2008). *Allostylops periconatus* Zheng, 1979, from the late Paleocene of China (Li and Ting, 1983) is distinguished in having a prominent pericone mesiolingual to the protocone on the upper molars. *Enantiostylops (Sinostylops) progressus* (Tang and Yan, 1976) was distinguished as a new genus by (Averianov, 2020, appendix 1) in having a strong internal invagination on the parastyle of M1 and M2. *Migrostylops rosella* (Tong and Wang, 2006) from the early Eocene Wutu Formation of China has a continuous lingual cingulum extending from the mesial face of the protocone to the distal face of the hypocone, a relatively weak, more labially positioned hypocone, and a relatively larger M3. *Bothriostylops notios* Zheng and Huang, 1986, from the late Paleocene of China is distinguished only by the lower dentition. Thus, the limited morphology preserved in

the M2 of PSS-MAE 673 most closely resembles that of *Palaeostylops*. Averianov (2020) provided a revised phylogeny for the Arctostylopidae that grouped *Palaeostylops*, *Arctostylops*, *Anatostylops*, and *Migrostylops* in a clade (Arctostylopinae) that excludes the other arctostyloids compared above.

As noted, the tooth measurements of PSS-MAE 673 are only approximate, but the teeth are clearly larger than in *Palaeostylops iturus*, comparable in size to *Palaeostylops macrodon*, and smaller than in *Arctostylops steini* and *Anatostylops zhaii*. Based on a sample of 21 specimens, Missiaen et al. (2012, table 1) calculated a mean value of 5.01 mm for maximum length of M2 in *P. macrodon*. The subequal length and width estimated for M2 in the Daus specimen (5 × 5 mm) is similar to, but slightly greater than, these dimensions in *Kazachostylops occidentalis* (4.6 × 4.5 mm in Averianov, 2020, table 1), but only a better-preserved specimen than PSS-MAE 673 will provide more meaningful size comparisons.

In summary, the incomplete features preserved in PSS-MAE 673 only allow a provisional identification of this new fossil as an indeterminate genus and species of arctostyloid. The specimen, as noted above, does show similarities to *Palaeostylops iturus*, a taxon that is abundantly represented in Gashatan faunas of Mongolia (see compilations in Kondrashov and Lucas, 2004; Missiaen et al., 2012). The Daus specimen may belong to a taxon larger than *Palaeostylops iturus*, but similar with respect to features of the lingual area of M2, including the well-developed crenulated cingulum.

*Arctostylops* was once thought to be an index taxon for the Asian Paleocene based on the presence of this genus also in the Paleocene of North America. As noted above, however, the Asian *Arctostylops* species, *A. iturus* (see Dashzeveg and Russell, 1988), has been re-assigned to *Palaeostylops iturus* (Cifelli et al., 1989; Kondrashov and Lucas, 2004), a species restricted to Asia, thus diminishing the role of this taxon as a global index fossil. The abundance of *Palaeostylops* in the Gashatan faunas may be biostratigraphically informative, at least within Asia, although arctostyloids are also represented in Bumbanian-aged faunas in China (Wang et al., 2008). The more recent higher taxonomic assignment of arctostyloids to Gliroformes (Missiaen et al., 2006) would obviate the long-held notion that the family belongs to the Notoungulata and part of a taxon of remarkable geographic range extending through Eurasia, North America, and South America. The taxonomic assignment by Missiaen et al. (2012), however, has not been entirely accepted. For example, Averianov (2020) recognized arctostyloids as belonging to the order Arctostylopida, which was erected by Cifelli et al. (1989), an assignment we adopt here, pending greater resolution of the matter.

## Discussion

We describe the lithology and paleontology of three new Naran Bulak Formation localities situated >90 km east of the type section (Gradziński et al., 1969; Dashzeveg and McKenna, 1977; Dashzeveg, 1988). The new site has yielded both invertebrates and fossil mammals, including some of the first reported skull material of two taxa: the gliroid *Gomphos* and a partial skull with a worn and damaged dentition that we provisionally identify as an indeterminate genus and species of an arctostyloid.



The Nemegt Basin is significant for being, along with the Lingcha Formation, Hengyang Basin, Hunan, China, one of the few localities in Asia that has continuous Paleocene–Eocene sedimentary rocks (Ting et al., 2003, p. 522). This feature, along with the superposition of the new localities on the highly fossiliferous Djadokhta Formation Cretaceous rocks at Ukhaa Tolgod (Dingus et al., 2008), makes additional exploration of these new deposits important for their potential to improve stratigraphy across the Cretaceous–Paleogene and Paleocene–Eocene boundaries in Asia.

Biostratigraphy has been the primary method of dating the Naran Bulak Formation because the formation lacks beds amenable to radiometric dating. Significant prior work exists naming Asian Land Mammal Ages (ALMAs) and fossils that characterize them. Noteworthy regarding the data in this paper is that the fossils collected in situ from the new Daus localities exhibit a mixed temporal signature when compared to prior findings. Lithologically, the localities are in the Naran Member (or ‘White Beds’) of the Naran Bulak Formation, which has been associated repeatedly with the Gashatan ALMA and is equivalent to the Nungshanian (Li and Ting, 1983), and assigned a Paleocene age (Kielan-Jaworowska and Dovchin, 1968; Gradziński, 1969; Szczechura, 1971; Shuvalov et al., 1974; Shishkin, 1975; Dashzeveg, 1982, 1988; Beard, 1998; Meng et al., 1998; Ting, 1998; Wang et al., 1998; Bowen et al., 2002, 2005; Ting et al., 2003; Clyde et al., 2008; Lopatin, 2020). The presence of *Archaeolambda*, known previously from Gashatan (and equivalent Nungshanian) or older rocks (Li and Ting, 1983; Ting, 1998; Wang et al., 1998; Bowen et al., 2002), suggests a Paleocene age for the new localities consistent with current hypotheses about the age of Naran Member beds. However, we note that Dashzeveg (1988, figs. 2, 4) had at one time proposed an Eocene age for *Archaeolambda* and that Lopatin (2020) underscored species-level differences for this taxon between Paleocene and Eocene beds. The presence of an arctostylopid with some dental similarities with the abundantly represented Gashatan genus *Palaeostylops* potentially also suggests a Paleocene age for the Daus fauna. However, this Paleocene temporal signature is contradicted by the presence of a taxon that has been recognized as a signature for the younger Bumban Member, the Bumbanian ALMA, and the early Eocene: *Gomphos elkema* (Dashzeveg, 1982, 1988; Dashzeveg and Russell, 1988; Meng et al., 2004). Additionally, *Pantolamodon* sp., recorded as an astragalus in the Daus beds, is known elsewhere in Asia from the late early-middle Eocene (Paepen et al., 2021). Finally, the presence of the ostracode *Limnocythere nemegtensis* also recently has been associated with Gashatan beds outside of Mongolia and considered Paleocene (Wang et al., 2019). However, this endemic Asian taxon has not yet met the criteria to be an index fossil of broad use. Thus, a mixed Paleocene and Eocene signal emerges from the new fossils recovered at this Naran Member locality. Alternative hypotheses have been proposed and may warrant further consideration, including that the Gashatan ALMA (Nungshanian) spans the Paleocene–Eocene boundary (Lucas, 1998) or that the Bumbanian faunas are late Paleocene (Beard, 1998).

Two diminutive skulls are among the remains found in this first exploration of the Daus localities. Like the Cretaceous Djadokhta Formation, the Naran Bulak beds at Daus appear, at least

preliminarily, to have a tendency to preserve small and delicate mammal skulls, a taphonomic signature that invites further exploration. Finally, more extensive study of the fluvio-lacustrine paleoecology suggested by these new localities, such as has been done for similar deposits described elsewhere on the Mongolian plateau in Inner Mongolia, People’s Republic of China (Van Itterbeek et al., 2007), will be necessary to better understand the paleoenvironment in which these early mammals existed.

## Acknowledgments

We are extremely grateful to the following people for expedition collaboration and research assistance: S. Goldberg, C. Merrill, and R. O’Leary. For helpful discussion on the manuscript we thank L. Antonietto, J. Meng, L.T. Holbrook, K.D. Rose, and S.P. Zack. This field research was accomplished with funding from the Margaret and Will Hearst Paleontological Research Fund and the Frick Laboratory Endowment at the AMNH. We thank the National Science Foundation for supporting this research through award DBI 0619559 for the AMNH SEM.

## Declaration of competing interests

The authors declare none.

## Data availability statement

Additional data is stored in the public database MorphoBank at project P4217: <http://dx.doi.org/10.7934/P4217>.

## References

- Asher, R.J., Meng, J., Wible J.R., McKenna, M.C., Rougier, G.W., Dashzeveg, D., and Novacek, M.J., 2005, Stem Lagomorpha and the antiquity of Glires: *Science*, v. 307, p. 1091–1094.
- Averianov, A.O., 1994, Early Eocene mimotonids of Kyrgyzstan and the problem of Mixodontia: *Acta Palaeontologica Polonica*, v. 39, p. 393–411.
- Averianov, A.O., 2020, Reappraisal of arctostylopid mammal *Kazachostylops occidentalis* from the late Paleocene of Kazakhstan and phylogenetic relationships within Arctostylopidia: *Journal of Paleontology*, v. 94, p. 568–579.
- Averianov, A.O., and Godinot, M., 2005, Ceratomorphs (Mammalia, Perissodactyla) from the early Eocene Andarak 2 locality in Kyrgyzstan: *Geodiversitas*, v. 27, p. 221–237.
- Badamgarav, D., and Reshetov, V.J., 1985, Paleontology and stratigraphy of the Paleogene of Transaltaic Gobi [translated from Russian: Палеонтология и стратиграфия Палеогена Заалтайской Гоби]: *The Joint Soviet-Mongolian Paleontological Expedition Transaction [Совместная Советско-Монгольская Палеонтологическая Экспедиция. Труды.]*, v. 25, p. 7–103.
- Bai, B., Wang, Y.Q., Li, Q., Wang, H.-B., Mao, F.-Y., Gong, Y.-X., and Meng, J., 2018, Biostratigraphy and diversity of Paleogene perissodactyls from the Erlan Basin of Inner Mongolia, China: *American Museum Novitates*, v. 3914, p. 1–60.
- Bai, B., Meng, J., Zhang, C., Gong, Y.X., and Wang, Y.Q., 2020, The origin of Rhinocerotidae and phylogeny of Ceratomorpha (Mammalia, Perissodactyla): *Communications Biology*, v. 3, p. 1–16.
- Baird, W., 1843, Notes on British Entomostraca: *The Zoologist*, v. 1, p. 193–197.
- Baird, W., 1845, Arrangement of the British Entomostraca, with a list of species, particularly noticing those which have as yet been discovered within the bounds of the Club: *History of the Berwickshire Naturalists’ Club*, v. 2, p. 145–158.
- Baird, W., 1850, Description of several new species of Entomostraca: *Proceedings of the Zoological Society of London*, v. 18, p. 254–257.
- Beard, K.C., 1998, East of Eden: Asia as an important center of taxonomic origination in mammalian evolution: *Bulletin of the Carnegie Museum of Natural History*, v. 34, p. 5–39.

- Bekhat, C., Naranbaatar, T., Badarch, G., and Davaa, U., 1999, Report on the results of the 1:200,000 scale geological mapping work carried out in Nemeget field in 1996–1997. (Topographic map K-47-IV, Y, YI, X, XI, XII and parts of XVI, XVII, XVIII) 1996–1997 [Translated from Mongolian], Гар бичмэл, Боть 1, Улаанбаатар., Ulaanbaatar.
- Bowen, G.J., Clyde, W.C., Koch, P.L., Ting, S., Alroy, J., Tsubamoto, T., Wang, Y., and Wang, Y., 2002, Mammalian dispersal at the Paleocene/Eocene boundary: *Science* v. 295, p. 2062–2065.
- Bowen, G.J., Koch, P.L., Meng, J., Ye, J., and Ting, S., 2005, Age and correlation of fossiliferous late Paleocene–early Eocene strata of the Erlian Basin, Inner Mongolia, China: *American Museum Novitates*, v. 3474, p. 1–26.
- Brady, G.S., 1868, A synopsis of recent British Ostracoda: *Intellectual Observer*, v. 12, p. 110–130.
- Cifelli, R.L., Schaff, C.R., and McKenna, M.C., 1989, The relationships of the Arctostylopidae (Mammalia): new data and interpretation: *Bulletin of the Museum of Comparative Zoology*, v. 152, p. 1–44.
- Clark, J.M., Norell, M.A., and Chiappe, L.M., 1999, An oviraptorid skeleton from the Late Cretaceous of Ukhaa Tolgod, Mongolia preserved in an avian-like brooding position over an oviraptorid nest: *American Museum Novitates*, v. 3265, p. 1–36.
- Clyde, W.C., Tong, Y., Snell, K.E., Bowen, G.J., Ting, S., Koch, P.L., Li, Q., Wang, Y., and Meng, J., 2008, An integrated stratigraphic record from the Paleocene of the Chijiang Basin, Jiangxi Province (China): implications for mammalian turnover and Asian block rotations: *Earth and Planetary Science Letters*, v. 269, p. 554–564.
- Cope, E.D., 1871, Descriptions of some new Vertebrata from the Bridger Group of the Eocene: *Proceedings of the American Philosophical Society*, v. 12, p. 460–465.
- Cope, E.D., 1873, On the short footed Ungulata of the Eocene of Wyoming: *Proceedings of the American Philosophical Society*, v. 13, p. 38–74.
- Cope, E.D., 1882, Two new genera of the Puerco Eocene: *The American Naturalist*, v. 16, p. 417–418.
- Cope, E.D., 1883, The ancestor of *Coryphodon*: *American Naturalist*, v. 17, p. 406–407.
- Dashzeveg, D., 1968, New data on the age of the lower Paleogene deposits of the Nemeget basin, Mongolia. [Translated from Russian: новые данные о возрасте нижнепалеогеновых отложений нэмэгтэинской котловины монголии]: Report of the Academy of Sciences of the USSR [Доклады Академии Наук СССР], v. 2, p. 415–417.
- Dashzeveg, D., 1977, On the first occurrence of *Hyopsodus* Leidy, 1870 (Mammalia, Condylarthra) in the People's Republic of Mongolia [translated from Russian: O pervoy nakhodke *Hyopsodus* Leidy, 1870 (Mammalia, Condylarthra) v Mongol'skoy Narodnoy Respublike]: *Transactions of the Joint Soviet-Mongolian Paleontological Expedition [Fauna, flora i biostatigrafiya mezozoya i kaynozoya Mongolii, Sovmestnaya Sov.-Mong. Nauchno-Issled. Geo. Eksped.]*, v. 4, p. 7–13.
- Dashzeveg, D., 1980, New pantodonts from the Eocene of Mongolia: *Paleontological Journal*, v. 1980, p. 108–115.
- Dashzeveg, D., 1982, La faune de mammifères du Paléogène inférieur de Naran-Bulak (Asie centrale) et ses corrélations avec l'Europe et l'Amérique du Nord: *Bulletin de la Société Géologique de France*, v. 24, p. 275–281.
- Dashzeveg, D., 1988, Holarctic correlation of non-marine Palaeocene-Eocene boundary strata using mammals: *Journal of the Geological Society*, v. 145, p. 473–478.
- Dashzeveg, D., and McKenna, M.C., 1977, Tarsioid primate from the early Tertiary of the Mongolian People's Republic: *Acta Palaeontologica Polonica*, v. 22, p. 119–137.
- Dashzeveg, D., and Russell, D.E., 1988, Palaeocene and Eocene Mixodontia (Mammalia, Glires) of Mongolia and China: *Paleontology*, v. 31, p. 129–164.
- Dashzeveg, D., Novacek, M.J., Norell, M.A., Clark, J.M., Chiappe, L.M., Davidson, A., McKenna, M.C., Dingus, L., Swisher III, C.C., and Altangerel, P., 1995, Extraordinary preservation in a new vertebrate assemblage from the Late Cretaceous of Mongolia: *Nature*, v. 374, p. 446–449.
- de Muizon, C., Billet, G., Argot, C., Ladevèze, S., and Goussard, F., 2015, *Alcidedorbignya inopinata*, a basal pantodont (Placentalia, Mammalia) from the early Palaeocene of Bolivia: anatomy, phylogeny and palaeobiology: *Geodiversitas*, v. 37, p. 397–634.
- Dingus, L., Loope, D.B., Dashzeveg, D., Swisher III, C.C., Minjin, C., Novacek, M.J., and Norell, M.A., 2008, The geology of Ukhaa Tolgod (Djadokhta Formation, Upper Cretaceous, Nemeget Basin, Mongolia): *American Museum Novitates*, v. 3616, p. 1–40.
- Flerov, K.K., 1952, Pantodonts collected by the Mongolian Paleontological Expedition Academy of Sciences of the USSR [Пантодонты (Pantodontia), собранные Монгольской Палеонтологической Экспедицией Академии Наук СССР]: *Proceedings of the Paleontological Institute [Труды Палеонтологического Института]* v. 41, p. 43–50.
- Gill, T., 1872, Arrangement of the families of mammals with analytical tables: *Smithsonian Miscellaneous Collections*, v. 11, p. 1–98.
- Gradziński, R., 1969, Results of the Polish-Mongolian palaeontological expeditions, Pt. II: sedimentation of the dinosaur-bearing Upper Cretaceous deposits of the Nemeget Basin: *Palaeontologia Polonica*, v. 21, p. 147–229.
- Gradziński, R., Kazmierczak, J., and Lefeld, J., 1969, Geographical and geological data from the Polish-Mongolian palaeontological expeditions: *Palaeontologia Polonica*, v. 18, p. 33–84.
- Granger, W., and Gregory, W.K., 1934, An apparently new family of amblypod mammals from Mongolia: *American Museum Novitates*, v. 720, p. 1–8.
- Hildebrand, M., 1978, Insertions and functions of certain flexor muscles in the hind leg of rodents: *Journal of Morphology*, v. 155, p. 111–122.
- Huang, X., 1977, *Archaeolambda* fossils from Anhui: *Vertebrata Palasiatica*, v. 15, p. 249–260.
- Khand, Y., 1987, Late Cretaceous and early Paleogene ostracans of the southern part of Mongolia and their stratigraphic significance [Translated from Russian: Поздне меловые и раннепалеогеновые остракоды южной части МНР и их стратиграфическое значение. Автореф. дис. канд. геол.-минерал. наук.]: *Autoreview*, p. 1–22.
- Kielan-Jaworowska, Z., 1968, *Archaeolambdidae* Flerov (Pantodontia) from the Paleocene of the Nemeget Basin, Gobi Desert: *Palaeontologia Polonica*, v. 19, p. 133–140.
- Kielan-Jaworowska, Z., and Dovchin, N., 1968, Narrative of the Polish-Mongolian palaeontological expeditions 1963–1965: *Paleontologica Polonica*, v. 19, p. 7–30.
- Kitts, D.B., 1956, American *Hyracotherium* (Perissodactyla, Equidae): *Bulletin of the American Museum of Natural History*, v. 110, p. 1–60.
- Klie, W., 1938, *Krebstiere oder Crustacea. III: Ostracoda, Muschelkrebse*, in Dahl, F., ed., *Die Tierwelt Deutschlands und der Angrenzenden Meeressteile*: Jena, Verlag von Gustave Fischer, p. 1–230.
- Kondrashov, P.E., and Lucas, S.G., 2004, *Palaeostylops iturus* from the upper Paleocene of Mongolia and the status of Arctostylopida (Mammalia, Eutheria): *Paleogene Mammals. New Mexico Museum Natural History and Science Bulletin*, v. 26, p. 195–204.
- Kraatz, B.P., Badamgarav, D., and Bibi, F., 2009, *Gomphos ellae*, a new mimotomid from the middle Eocene of Mongolia and its implications for the origin of Lagomorpha: *Journal of Vertebrate Paleontology*, v. 29, p. 576–583.
- Latreille, P.A., 1806, *Genera crustaceorum et insectorum secundum ordinem naturalem in familia disposita, iconibus exemplarum plurimis explicata*: Paris and Strasbourg, Amand Koenig, v. 1, 302 p.
- Leidy, J., 1870, Abstract of remarks made before a meeting of the Academy of Natural Sciences of Philadelphia, October 4th, 1870: *Proceedings of the Academy of Natural Sciences of Philadelphia*, v. 22, p. 109–110.
- Li, C.-K., 1977, Paleocene eurymylids (Anagalida, Mammalia) of Quianshan, Anhui: *Vertebrata Palasiatica*, v. 15, p. 103–118.
- Li, C.-K., and Ting, S., 1983, The Paleogene mammals of China: *Bulletin of the Carnegie Museum of Natural History*, v. 21, p. 1–93.
- Li, C.-K., Wilson, R.W., Dawson, M.R., and Krishtalka, L.T., 1987, The origin of rodents and lagomorphs, in Genoways H.H., ed., *Current Mammals*: New York, Plenum, p. 97–108.
- Li, Q., Wang, Y.Q., and Fostowicz-Freluk, Ł., 2016, Small mammal fauna from Wulanxuhui (Nei Mongol, China) implies the Irindmanhan-Sharamurian (Eocene) faunal turnover: *Acta Palaeontologica Polonica*, v. 61, p. 759–776.
- Linnaeus, C., 1758, *Systema Naturae*, Editio X. [Systema naturae per regna tria naturae, secundum classes, ordines, genera, species, cum characteribus, differentiis, synonymis, locis. Tomus I. Editio decima, reformata]: Holmiae, Laurentii Salvii, 824 p.
- Lopatin, A.V., 2020, A review of the Mesozoic and Cenozoic mammals of Mongolia: *Paleontological Journal*, v. 54, p. 779–808.
- Lucas, S.G., 1998, Fossil mammals and the Paleocene/Eocene series boundary in Europe, North America, and Asia, in Aubry, M.-P., Lucas, S.G., and Berggren, W.A., eds., *Late Paleocene–Early Eocene Climatic and Biotic Events in the Marine and Terrestrial Records*: New York, Columbia University Press, p. 451–500.
- Luckett, W.P., 1985, Superordinal and intraordinal affinities of rodents: developmental evidence from the dentition and placentation. in Luckett, W.P., and Hartenberger, J.-L., eds., *Evolutionary Relationships Among Rodents*: Boston, MA, Springer, p. 227–276.
- Luckett, W.P., and Hartenberger, J.-L., 1993, Monophyly or polyphyly of the order Rodentia: possible conflict between morphological and molecular interpretations: *Journal of Mammalian Evolution*, v. 1, p. 127–147.
- Martin, G.P.R., 1940, Ostracoden des norddeutschen Purbeck und Wealden: *Senckenbergiana*, v. 22, p. 275–361.
- Martin, G.P.R., 1958, Über die systematische Stellung der Gattung *Cypridea* Posquet (Ostracoda), nebst Beschreibung der Wealden-Basis-Ostracode *C. buxtorfi* n. sp.: *Neues Jahrbuch für Geologie und Paläontologie, Monatshefte*, v. 7, p. 312–320.
- Matthew, W.D., 1909, The Carnivora and Insectivora of the Bridger Basin, middle Eocene: *Memoirs of the American Museum of Natural History*, v. 9, p. 289–567.

- Matthew, W.D., 1915, A revision of the lower Eocene Wasatch and Wind River faunas. Part IV. Entelonychia, primates, Insectivora: Bulletin of the American Museum of Natural History, v. 34, p. 429–483.
- Matthew, W.D., 1937, Paleocene faunas of the San Juan Basin, New Mexico: Transactions of the American Philosophical Society, v. 30, p. 1–510.
- Matthew, W.D., and Granger, W., 1925, Fauna and correlation of the Gashato Formation of Mongolia: American Museum Novitates, v. 189, p. 1–12.
- Matthew, W.D., Granger, W., and Simpson, G.G., 1929, Additions to the fauna of the Gashato Formation of Mongolia: American Museum Novitates, v. 376, p. 1–12.
- McKenna, M.C., and Bell, S.K., 1997, Classification of Mammals Above the Species Level: New York, Columbia University Press, 640 p.
- Meisch, C., 2000, Freshwater Ostracoda of Western and Central Europe: Heidelberg, Spektrum Akademischer Verlag GmbH, 522 p.
- Meng, J., Zhai, R., and Wyss, A.R., 1998, The late Paleocene Bayan Ulan Fauna of Inner Mongolia, China: Bulletin of the Carnegie Museum of Natural History, v. 34, p. 148–185.
- Meng, J., Hu, Y., and Li, C., 2003, The osteology of *Rhombomylus* (Mammalia, Glires): implications for phylogeny and evolution of Glires: Bulletin of the American Museum of Natural History, v. 275, p. 1–247.
- Meng, J., Bowen, G.J., Ye, J., Koch, P.L., Ting, S., Li, Q., and Jin, X., 2004, *Gomphos elkema* (Glires, Mammalia) from the Erlian Basin: evidence for the early Tertiary Bumbanian Land Mammal Age in Nei-Mongol, China: American Museum Novitates, v. 3425, p. 1–24.
- Meng, J., Wyss, A.R., Hu, Y., Wang, Y., Bowen, G.J., and Koch, P.L., 2005, Glires (Mammalia) from the late Paleocene Bayan Ulan locality of Inner Mongolia: American Museum Novitates, v. 3473, p. 1–25.
- Meng, J., Kraatz, B.P., Wang, Y., Ni, X., Gebo, D.L., and Beard, K.C., 2009, A new species of *Gomphos* (Glires, Mammalia) from the Eocene of the Erlian Basin, Nei Mongol, China: American Museum Novitates, v. 3670, p. 1–11.
- Missiaen, P., Smith, T., Guo, D.-Y., Bloch, J.I., and Gingerich, P.D., 2006, Asian gliriform origin for arctostylopid mammals: Naturwissenschaften, v. 93, p. 407–411.
- Missiaen, P., Escarguel, G., Hartenberger, J.-L., and Smith, T., 2012, A large new collection of *Palaeostylops* from the Paleocene of the Flaming Cliffs area (Ulan-Nur Basin, Gobi Desert, Mongolia), and an evaluation of the phylogenetic affinities of Arctostylopidae (Mammalia, Gliriformes): Geobios v. 45, p. 311–322.
- Müller, G.W., 1894, Fauna und Flora des Golfes von Neapel und der Angrenzenden Meeres-Abschnitte. 21. Monographie: Ostracoden: Berlin, Verlag von R. Friedländer & Sohn, 404 p.
- Nessov, L.A., 1987, Rezultaty poiskov i issledovaniya Melovykh i Rannepaleogenovykh mlekopitayushikh na territorii SSSR [Results of search and study of Cretaceous and early Paleogene mammals on the territory of the USSR]: Ezhegodnik Vsesoyuznogo Paleontologicheskogo Obshchestva, v. 30, p. 199–218.
- Neustrueva, I.Y., Sinitisa, S.M., Khand, Y., and Melnikova, L.M., 2005, Palaeontology of Mongolia: Late Mesozoic and Paleogene Ostracoda: Moscow, Nauka, 118 p. [in Russian]
- Norell, M.A., Clark, J.M., Dashzeveg, D., Barsbold, R., Chiappe, L.M., Davidson, A.R., McKenna, M.C., and Novacek, M.J., 1994, A theropod dinosaur embryo and the affinities of the Flaming Cliffs dinosaur eggs: Science, v. 266, p. 779–782.
- Novacek, M.J., Rougier, G.W., Wible, J.R., McKenna, M.C., Dashzeveg, D., and Horowitz, I., 1997, Epipubic bones in eutherian mammals from the Late Cretaceous of Mongolia: Nature, v. 389, p. 483–486.
- O’Leary, M.A., and Rose, K.D., 1995, Postcranial skeleton of the early Eocene mesonychiid *Pachyaena* (Mammalia: Mesonychia): Journal of Vertebrate Paleontology, v. 15, p. 401–430.
- O’Leary, M.A., Bloch, J.I., Flynn, J.J., Gaudin, T.J., Giallombardo, A., et al., 2013, The placental mammal ancestor and the post-K–Pg radiation of placentals: Science, v. 339, p. 662–667.
- Owen, R., 1837, On the structure of the brain of marsupial animals: Philosophical Transactions of the Royal Society of London, v. 127, p. 87–96.
- Paepen, M., Hong, L., Yan, S., and Smith, T., 2021, A late early to early middle Eocene mammal assemblage from Bayan Ulan (Inner Mongolia, China): implication for the reassessment of the Arshantan Asian Land Mammal Age: Geobios, v. 66, p. 177–191.
- Pol, D., and Norell, M.A., 2004, A new crocodyliform from Zos Canyon, Mongolia: American Museum Novitates, v. 3445, p. 1–36.
- Radinsky, L.B., 1965, Early Tertiary Tapiroidea of Asia: Bulletin of the American Museum of Natural History, v. 129, p. 181–264.
- Reshetov, V.Y., 1979, [Early Tertiary tapiroids of Asia]: Trudy Sovmestnoi Sovetsko-Mongol’skoi Paleontologicheskoi Ekspeditsii, v. 11, p. 1–144. [in Russian]
- Russell, D.E., and Zhai, R.J., 1987, The Paleogene of Asia: mammals and stratigraphy: Memoires du Museum National d’Histoire Naturelle, v. 52, p. 1–488.
- Sames, B., 2011, Early Cretaceous Crypridea Bosquet 1852 in North America and Europe: Micropaleontology, v. 57, p. 345–431.
- Schlosser, M., 1923, Mammalia. Säugetiere, in Broili, F., and Schlosser, M., eds., K.A. von Zittel, Grundzüge der Paläontologie (Paläozoologie). Neubearbeitet: München, Oldenbourg, p. 402–689.
- Shevyreva, N.S., Chkhikvadze, V.M., and Zhegallo, V.I., 1975, New data on the vertebrate fauna of the Gashato Formation, Mongolian People’s Republic [Новые данные о фауне позвоночных местонахождения Гашато (Монгольская Народная Республика)]: Bulletin of the Academy of Sciences of the Georgian SSR [Сообщения Академии Наук Грузинской ССР], v. 77, p. 225–228.
- Shishkin, M.A., 1975, Stratigraphy and taphonomy of the upper Paleocene locality of vertebrates Naran-Bulak (Southern Gobi Mongolian People’s Republic) [translated from Russian: Stratigraphia i taphonomia verhnepaleotsenovogo mestonahojdeniya posvonochnyh Naran-Bulak (South Gobi MNR): Iskopaemaya fauna i flora Mongolii], p. 230–249, Fossil fauna and flora of Mongolia: Transactions of the Joint Soviet-Mongolian Paleontological Expedition v. 2, p. 230–249.
- Shuvalov, B.F., Reshetov, B.Y., and Barsbold, R., 1974, On the stratigraphic section of the lower Paleogene in the southwest of the Mongolian People’s Republic [Translated from Russian: О стратигическом разрезе нижнего палеогена на юго-западе мнр] Fauna and biostratigraphy of the Mesozoic and Cenozoic of Mongolia: Transactions of the Joint Soviet-Mongolian Paleontological Expedition, v. 1, p. 265–267.
- Simons, E.L., 1960, The Paleocene Pantodonta: Transactions of the American Philosophical Society, v. 50, p. 3–99.
- Szczeczura, J., 1971, Freshwater ostracods from the Paleocene of the Nemegt Basin, Gobi Desert, Mongolia: Palaeontologica Polonica, v. 15, p. 87–97.
- Tang, Y.J., and Yan, D.F., 1976, Notes on some mammalian fossils from the Paleocene of Qianshan and Xuancheng, Anhui: Vertebrata Palasiatica, v. 14, p. 91–99.
- Ting, S., 1998, Paleocene and early Eocene land mammal ages of Asia, in Beard, C.K., and Dawson, M.R., eds., Dawn of the Age of Mammals in Asia: Bulletin of the Carnegie Museum of Natural History, v. 34, p. 124–147.
- Ting, S., Bowen, G.J., Koch, P.L., Clyde, W.C., Wang, Y., Wang, Y., and McKenna, M.C., 2003, Biostratigraphic, chemostratigraphic, and magnetostratigraphic study across the Paleocene-Eocene boundary in the Hengyan Basin, Hunan, China: Geological Society of America Special Paper v. 369, p. 521–535.
- Tong, Y., and Wang, J., 2006, Fossil mammals from the early Eocene Wutu Formation of Shandong Province: Palaeontologia Sinica, n. ser. C, v. 28, p. 1–195.
- Van Itterbeeck, J., Missiaen, P., Folie, A., Markevich, V.S., Van Damme, D., Gou, D.-Y., and Smith, T., 2007, Woodland in a fluvio-lacustrine environment on the dry Mongolian Plateau during the late Paleocene: evidence from the mammal bearing Subeng section (Inner Mongolia, P.R. China): Palaeogeography, Palaeoclimatology, Palaeoecology, v. 243, p. 55–78.
- Van Morkhoven, F.P.C.M., 1963, Post-Paleozoic Ostracoda. Their Morphology, Taxonomy and Economic Use. Volume II: Amsterdam, Elsevier, 478 p.
- Wang, J.W., 1988, A new genus of ceratomorphs (Mammalia) from middle Eocene of China: Vertebrata Palasiatica, v. 26, p. 20–34.
- Wang, Y.-Q., Hu, Y.M., Zhou, M.Z., and Li, C.K., 1998, Chinese Paleocene mammal faunas and their correlation: Bulletin of Carnegie Museum of Natural History, v. 34, p. 89–123.
- Wang, Y.-Q., Meng, J., Ni, X.-J., and Beard, K.C., 2008, A new early Eocene arctostylopid (Arctostylopidae, Mammalia) from the Erlian Basin, Nei Mongol (Inner Mongolia), China: Journal of Vertebrate Paleontology, v. 28, p. 553–558.
- Wang, Y.-Q., Meng, J., Beard, C.K., Li, Q., Ni, X.J., Gebo, D.L., Bai, B., Jin, X., and Li, P., 2010, Early Paleogene stratigraphic sequences, mammalian evolution and its response to environmental changes in Erlian Basin, Inner Mongolia, China: Science China—Earth Sciences, v. 53, p. 1918–1926.
- Wang, Y.-Q., Meng, J., Jin, X., Beard, K.C., Bai, B., Li, P., Ni, X.-J., Li, Q., and Gebo, D.L., 2011, Early Eocene perissodactyls (Mammalia) from the Upper Nomogen Formation of the Erlian Basin, Nei Mongol, China: Vertebrata Palasiatica, v. 49, p. 123–140.
- Wang, Y.-Q., Li, Q., Bai, B., Jin, X., Mao, F., and Meng, J., 2019, Paleogene integrative stratigraphy and timescale of China: Science China Earth Sciences v. 62, p. 287–309.
- Woodburne, M.O., and Swisher III, C.C., 1995, Land mammal high-resolution geochronology, intercontinental overland dispersals, sea level, climate and vicariance, in Berggren, W.A., Kent, D.V., Aubry, M.-P., and Hardenbol, J., eds., Geochronology Time Scales and Global Stratigraphic Correlation: SEPM Special Publication, v. 54, p. 335–365.
- Zhai, R., 1978, The mammalian fauna of the Shisanjianfang Formation and its significance toward paleobiogeographic studies [translated from Chinese]: Memoirs of the Institute of Vertebrate Paleontology and Paleoanthropology, Academia Sinica, Series 1, v. 13, p. 107–115.
- Zhao, S.D., 1985, Ostracods from the Upper Cretaceous and lower Tertiary in the Erlian Basin, Nei Mongol, in Micropaleontological Society of China,



- ed., Selected Works on Micropalaeontology: Beijing, Science Press, p. 109–118.
- Zheng, J., 1979, Notoungulata from the Paleocene of Jiangsu, South China [translated from Chinese], in Institute of Vertebrate Paleontology, Paleanthropology & Nanjing Institute of Paleontology, eds., The Mesozoic and Cenozoic Red Beds of South China: Beijing, Science Press, p. 387–394.
- Zheng, J., and Huang, X., 1986, New arctostyloids (Notoungulata, Mammalia) from the late Paleocene of Jiangxi: *Vertebrata Pal Asiatica*, v. 24, p. 121–128.

Accepted: 9 September 2022